# Peptide Lipidation in Lysophospholipid Micelles and Lysophospholipid-Enriched Membranes

Vian S Esmaeil,[1,2] Hannah M Britt,[1,3] Jackie A Mosely[4] and John M Sanderson[1]

1. Chemistry Department, Durham University, Durham, DH1 3LE, UK
2. Current address: Chemistry Department, Soran University, Kurdistan Region, Iraq
3. Current address: Institute of Structural & Molecular Biology, University College London, Gower Street, London, WC1E 6BT
4. National Horizons Centre, School of Health & Life Sciences, Teesside University, Darlington DL1 1HG

## Supporting Information: Contents

### Chromatograms and Mass Spectra



### Other Figures



### Tables



### References

## Supporting Information: Chromatograms

### 1. Melittin + 1 Acyl Group

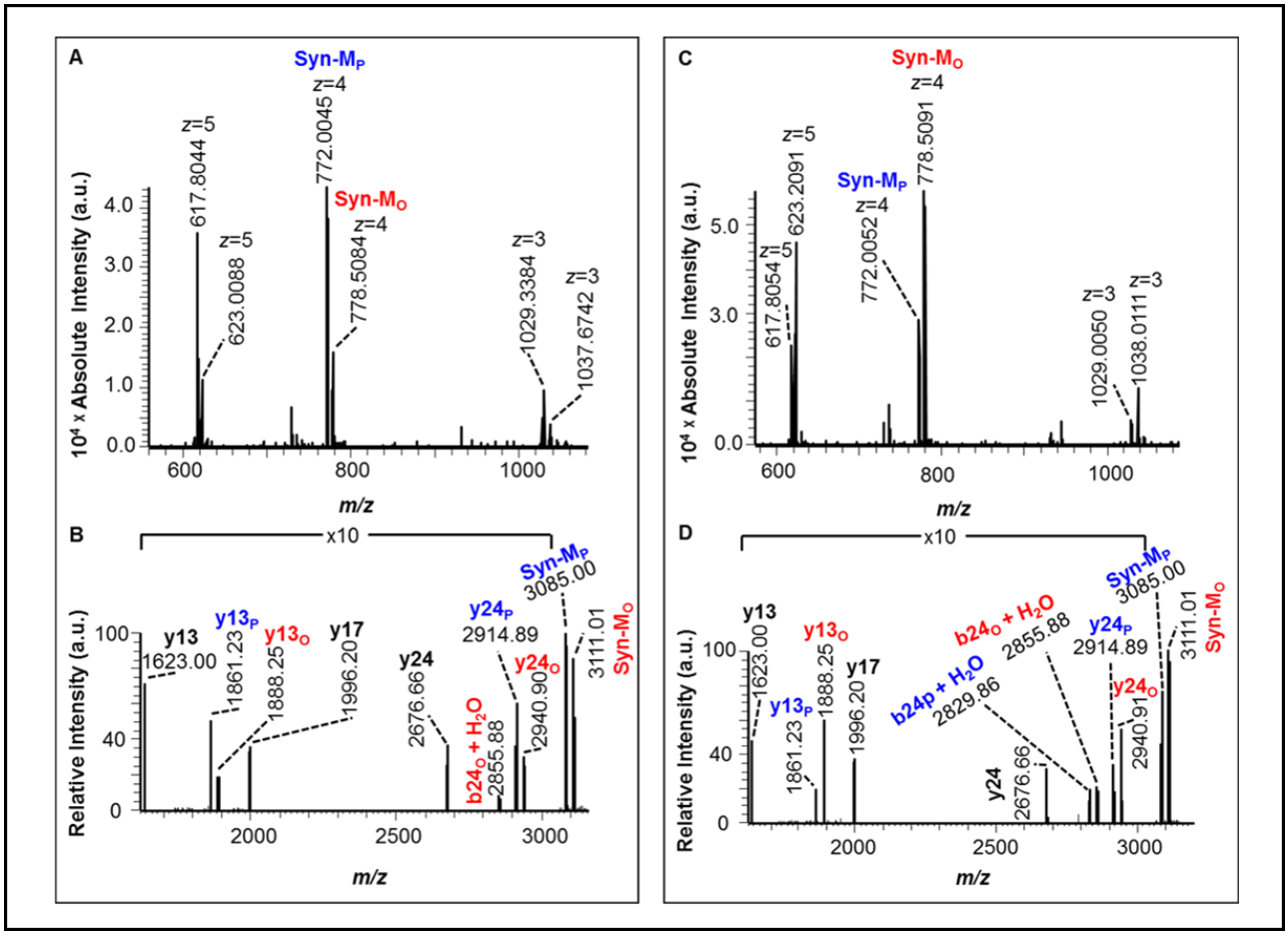


**Figure S1.** Mass spectra for melittin modified with a single acyl group. All were obtained from analyses of melittin incubated with mixtures of lysolipid/lipid, 1:1 (Fig. 3, main article; RT = 7.9–9.8 min). (B) and (D) are deconvolved from (A) and (C) respectively. (A) and (B): melittin + 50:50 PPC:DOPC. Assignments are in Table S3. (C) and (D): melittin + 50:50 OPC:DPPC. Assignments are in Table S4. Ions labeled Syn-$M_P$ and Syn-$M_O$ correspond respectively to the addition of a single palmitoyl or oleoyl group. Fragment ions (*b* and *y*) modified with an acyl group are labelled with a P or O subscript according to the identity of the acyl group.

## 2. Melittin + 2 Acyl Groups

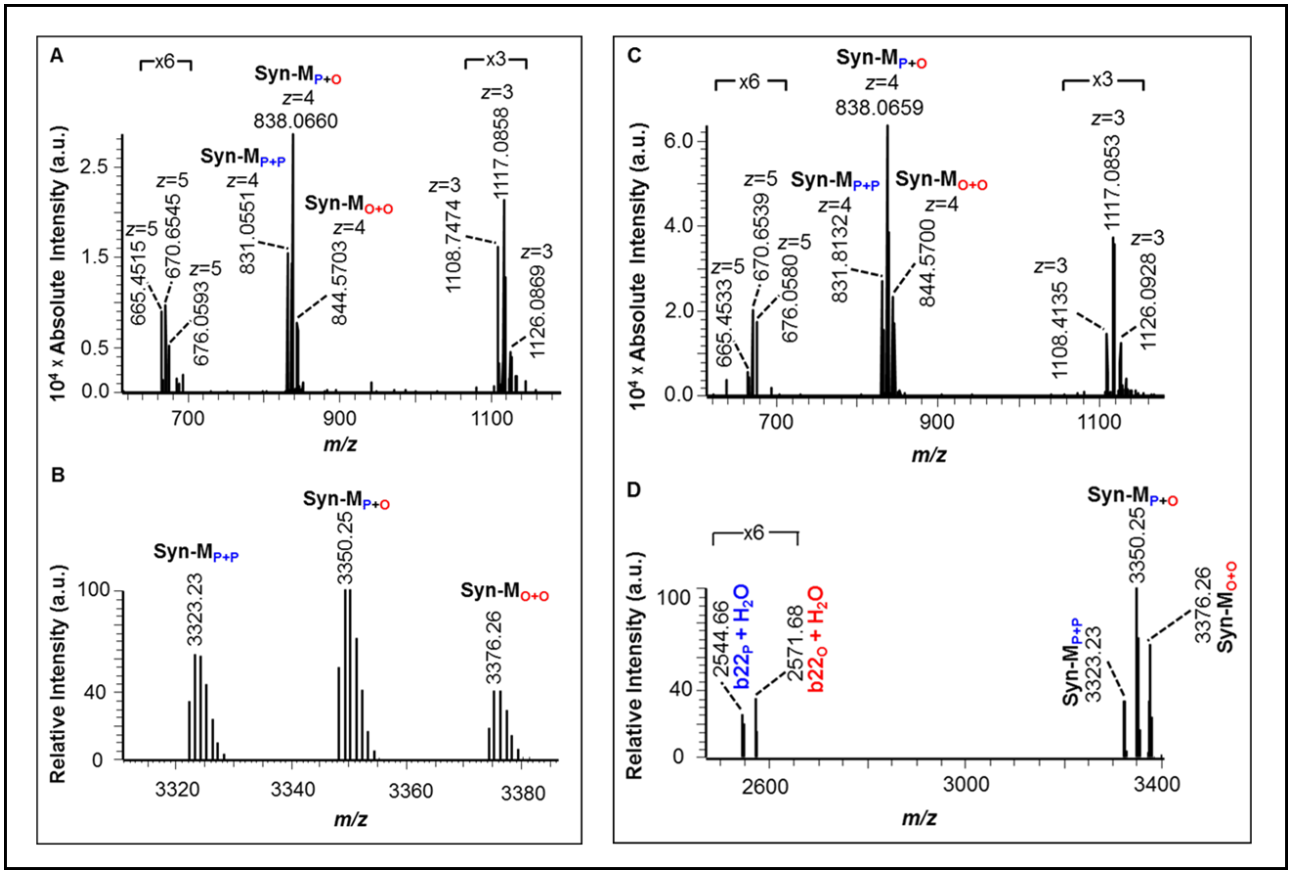


**Figure S2.** Mass spectra for melittin modified with 2 acyl groups. All were obtained following incubation at 37 °C over 168 h using the LC-MS conditions in Fig. 2 (main article). (B) and (D) are deconvolved from (A) and (C) respectively. (A) and (B): melittin + 50:50 PPC:DOPC, RT = 9.5–11.8 min. Assignments are in Table S3. (C) and (D): melittin + 50:50 OPC:DPPC, RT = 9.6–11.9 min. Assignments are in Table S4. Ions labeled Syn-$M_{P+P}$, Syn-$M_{P+O}$ and Syn-$M_{O+O}$ correspond respectively to the double addition of acyl groups (2 palmitoyl, 1 oleoyl + 1 palmitoyl or 2 oleoyl respectively). Fragment ions (*b* and *y*) modified with an acyl group are labelled with a P or O subscripts according to the identity of the acyl group.

## 3. Melittin + 3 Acyl Groups

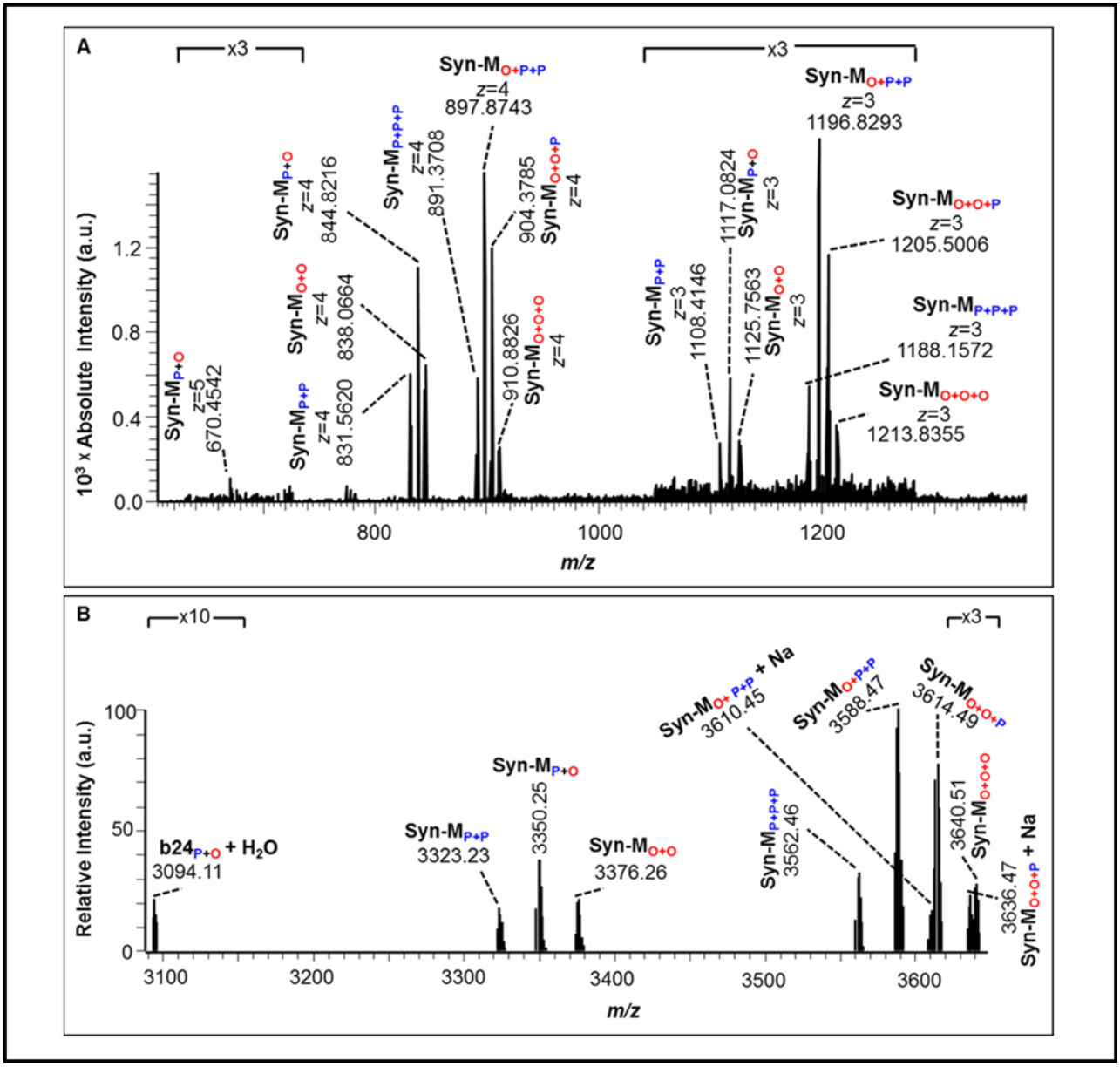


**Figure S3.** Mass spectra for melittin modified with 3 acyl groups following incubation with 50:50 PPC:DOPC at 37 °C over 168 h using the LC-MS conditions in Fig. 2 (main article), RT = 17–19 min. (A) mass spectrum over different charge states. The spectrum includes some ions with 2 acyl groups that were formed by in-source fragmentation of melittin + 3 acyl groups. Syn-$M_{P+P+P}$, Syn-$M_{O+P+P}$, Syn-$M_{O+O+P}$ and Syn-$M_{O+O+O}$ correspond respectively to the triple addition of acyl groups (3 palmitoyl, 1 oleoyl + 2 palmitoyl, 2 oleoyl + 1 palmitoyl, or 3 oleoyl respectively). Other peaks are labelled as per Fig. S2. Assignments are in Table S3.

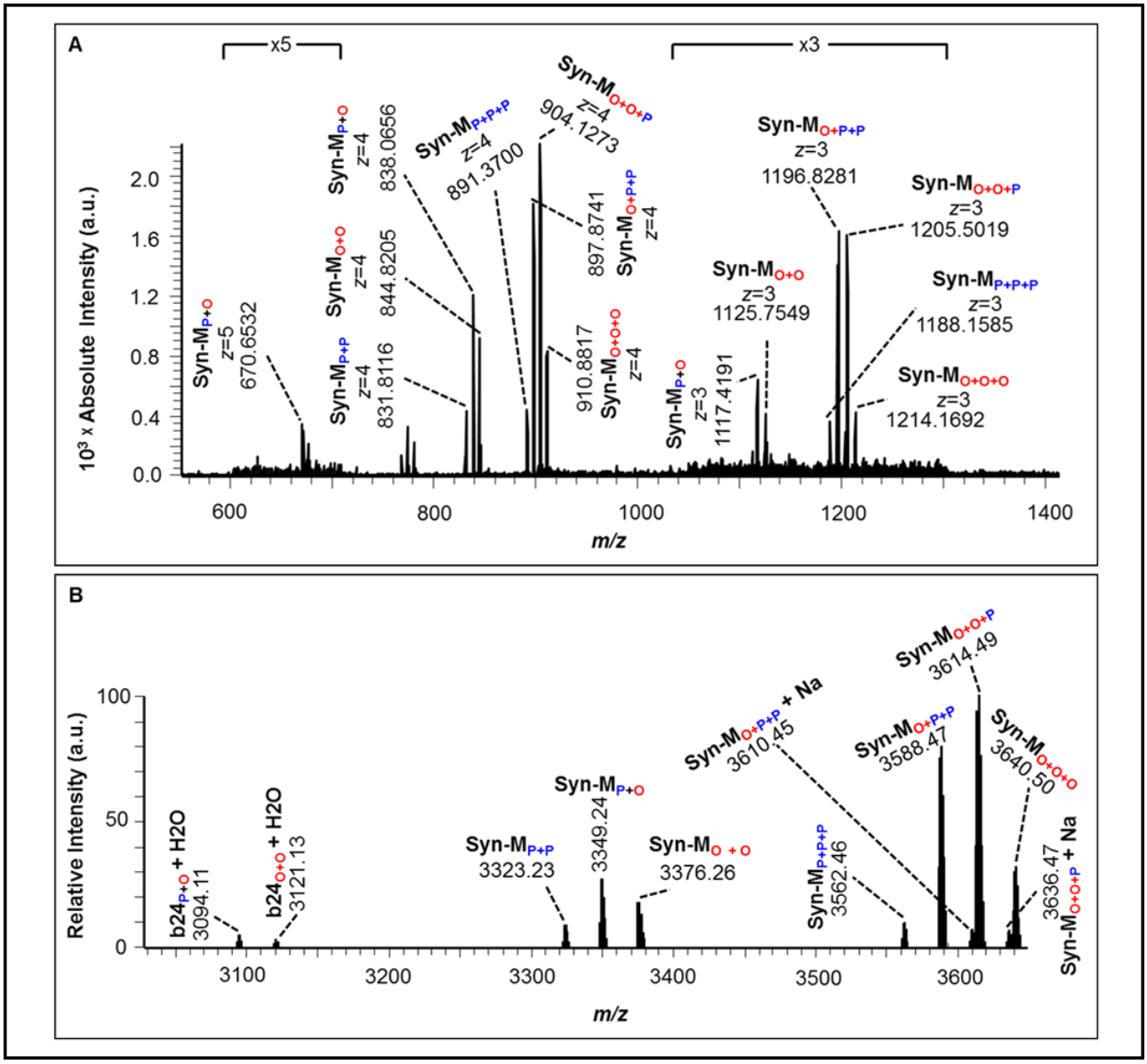


**Figure S4.** Mass spectra for melittin modified with 3 acyl groups following incubation with 50:50 OPC:DPPC at 37 °C over 168 h using the LC-MS conditions in Fig. 2 (main article), RT = 17–19 min. (A) mass spectrum over different charge states. The spectrum includes some ions with 2 acyl groups that were formed by in-source fragmentation of melittin + 3 acyl groups. Syn-M$_{P+P+P}$, Syn-M$_{O+P+P}$, Syn-M$_{O+O+P}$ and Syn-M$_{O+O+O}$ correspond respectively to the triple addition of acyl groups (3 palmitoyl, 1 oleoyl + 2 palmitoyl, 2 oleoyl + 1 palmitoyl, or 3 oleoyl respectively). Other peaks are labelled as per Fig. S2. Assignments are in Table S4.

## 4. Double Acylated (2 × Palmitoyl) Melittin

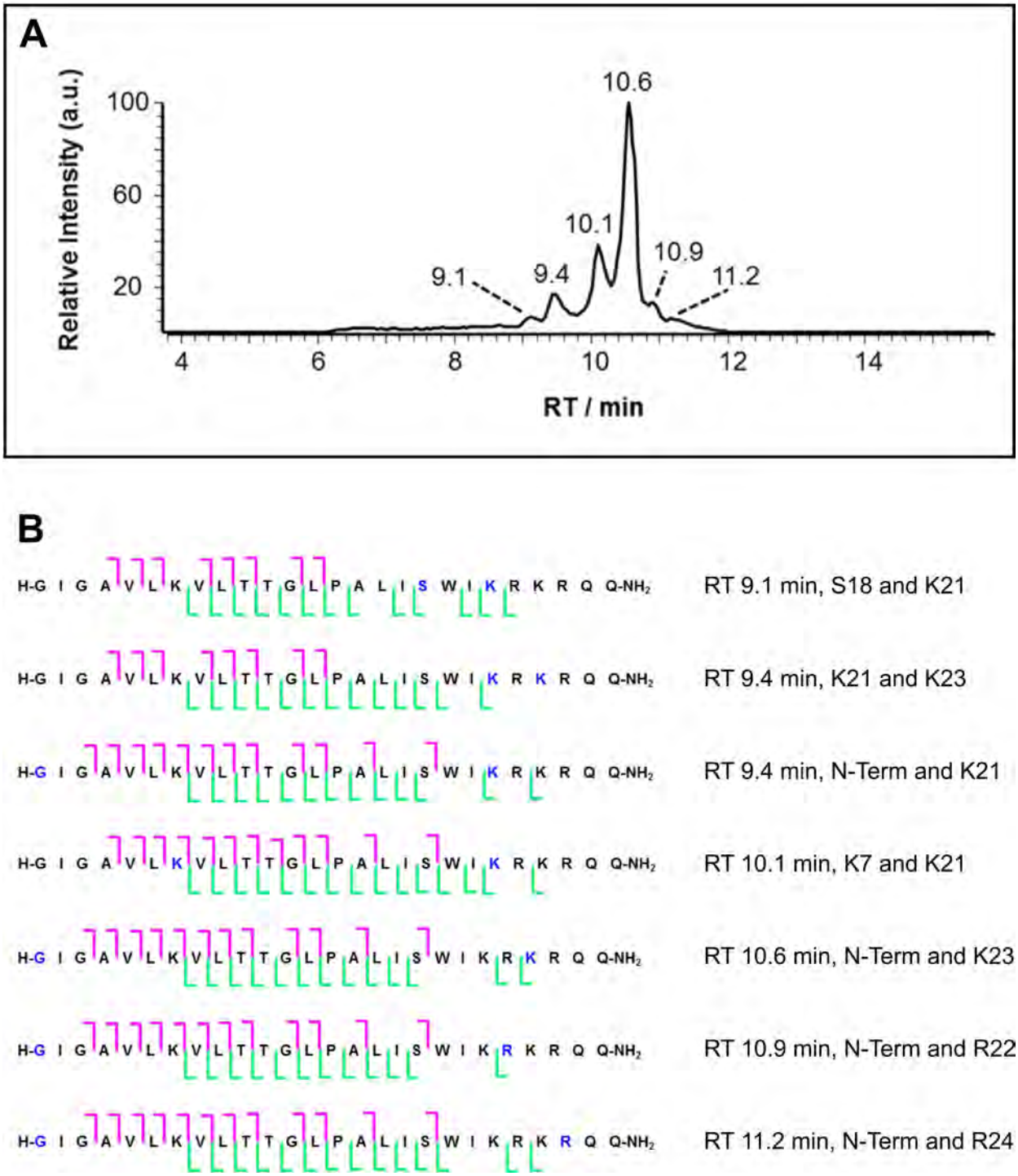


**Fig. S5**. **A**. TIC from CID fragmentation of melittin modified by two palmitoyl groups at *m*/*z* 832 (*z* = 4) on ESI-LTQ-MS (LTQFT). Modified melittin was prepared by incubation of synthetic melittin with 50:50 PPC:DOPC over 168 h at 37 °C. **B**. Sequence ladders summarising *y*-type (green) and *b*-type (magenta) ions observed following fragmentation of double palmitoylated precursor ions of *m*/*z* 832 (*z* = 4) by CID (LTQ). Acylation sites are highlighted in blue. Full details are provided in Figs. S6-S8 and Tables S5-S11.

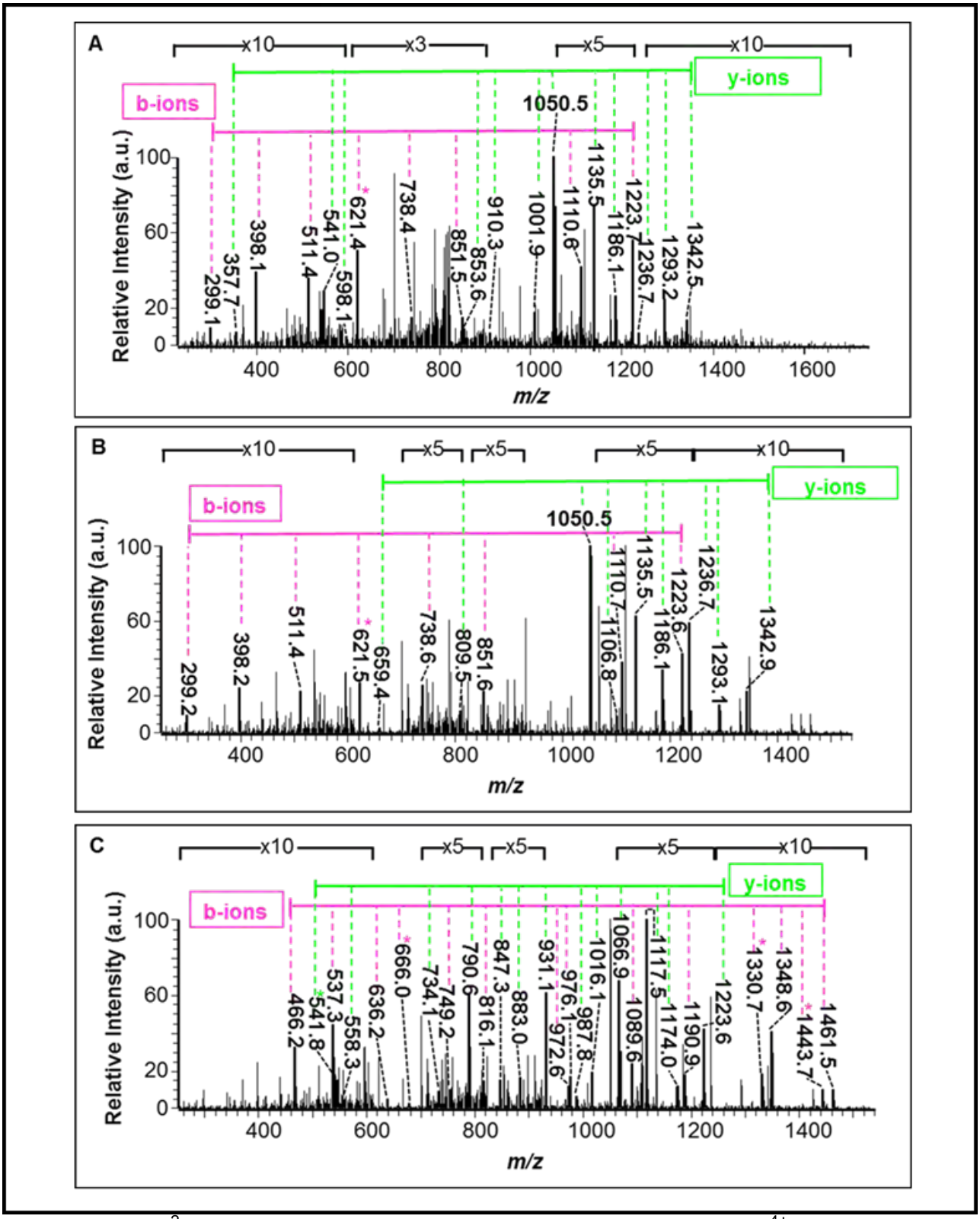


**Fig. S6**. LC-MS$^2$ spectra of the precursor ion at *m/z* 832 for $[M_{P+P} + 4H]^{4+}$ at 9.1 min (A) and 9.4 min (B and C; Fig. S5). The *y*-type and *b*-type ions are shown on each spectrum. The peaks labelled with an asterisk represent: *m/z* 621.4, $[(b13 + H_2O) + 2H]^{2+}$; *m/z* 541.8, $[(y4 – NH_3) + H]^+$; *m/z* 666.0, $[(b12_P – H_2O) + 2H]^{2+}$; *m/z* 1330.7, $[(b12_P – H_2O) + H]^+$; *m/z* 1443.7, $[(b13_P – H_2O) + H]^+$. Data are tabulated in Tables S5-S7.

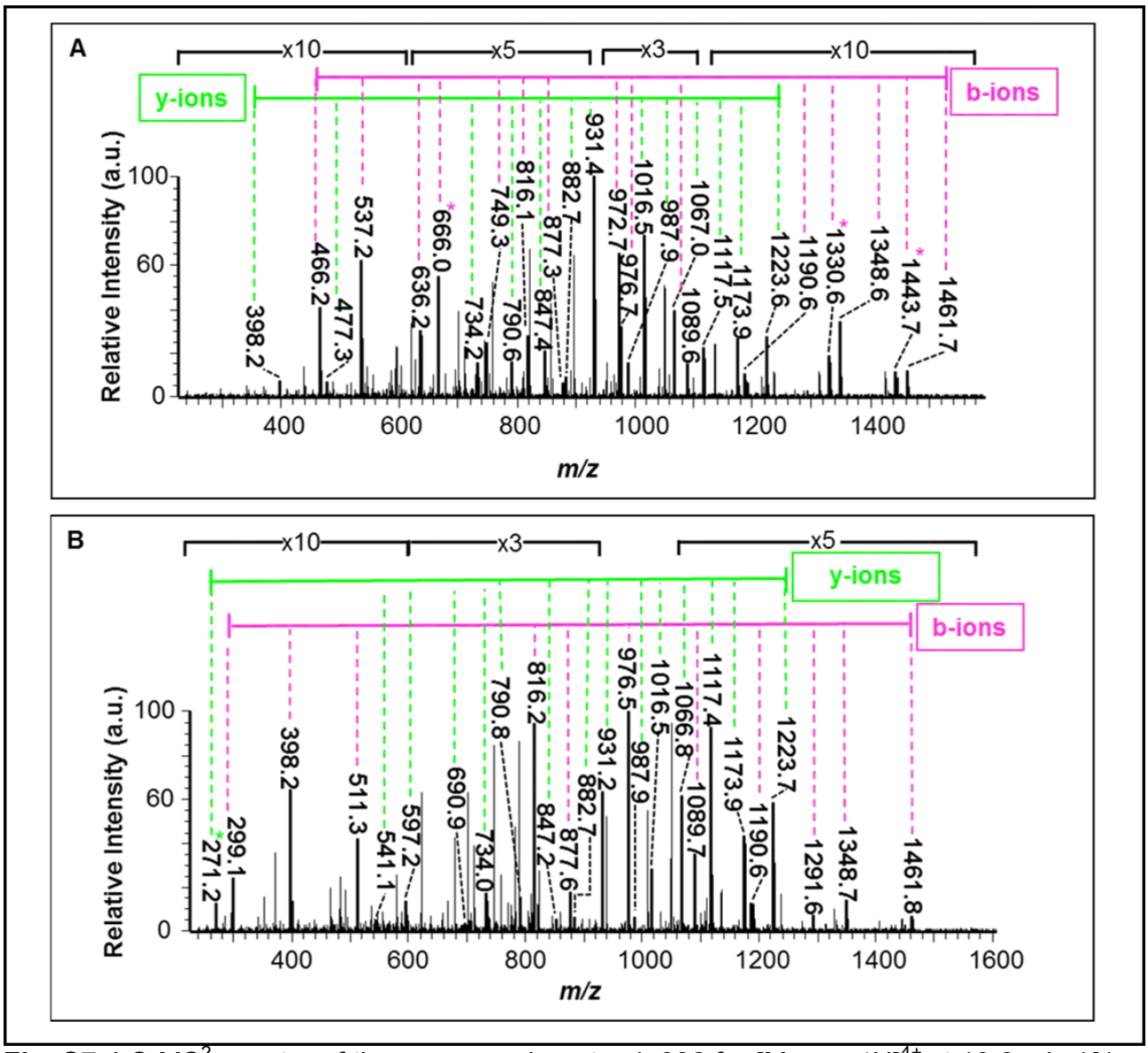


**Fig. S7**. LC-MS$^2$ spectra of the precursor ion at *m/z* 832 for $[M_{P+P} + 4H]^{4+}$ at 10.6 min (**A**) and 10.1 min (**B** and C; Fig. S5). The *y*-type and *b*-type ions are shown on each spectrum. The peaks labelled with an asterisk represent: *m/z* 621.4, $[(b13 + H_2O) + 2H]^{2+}$; *m/z* 271.2, $[(y4 – NH_3) + 2H]^{2+}$; *m/z* 666.0, $[(b12_P – H_2O) + 2H]^{2+}$; *m/z* 1330.6, $[(b12_P – H_2O) + H]^{+}$; *m/z* 1443.7, $[(b13_P – H_2O) + H]^{+}$. Data are tabulated in Tables S8 and S9.

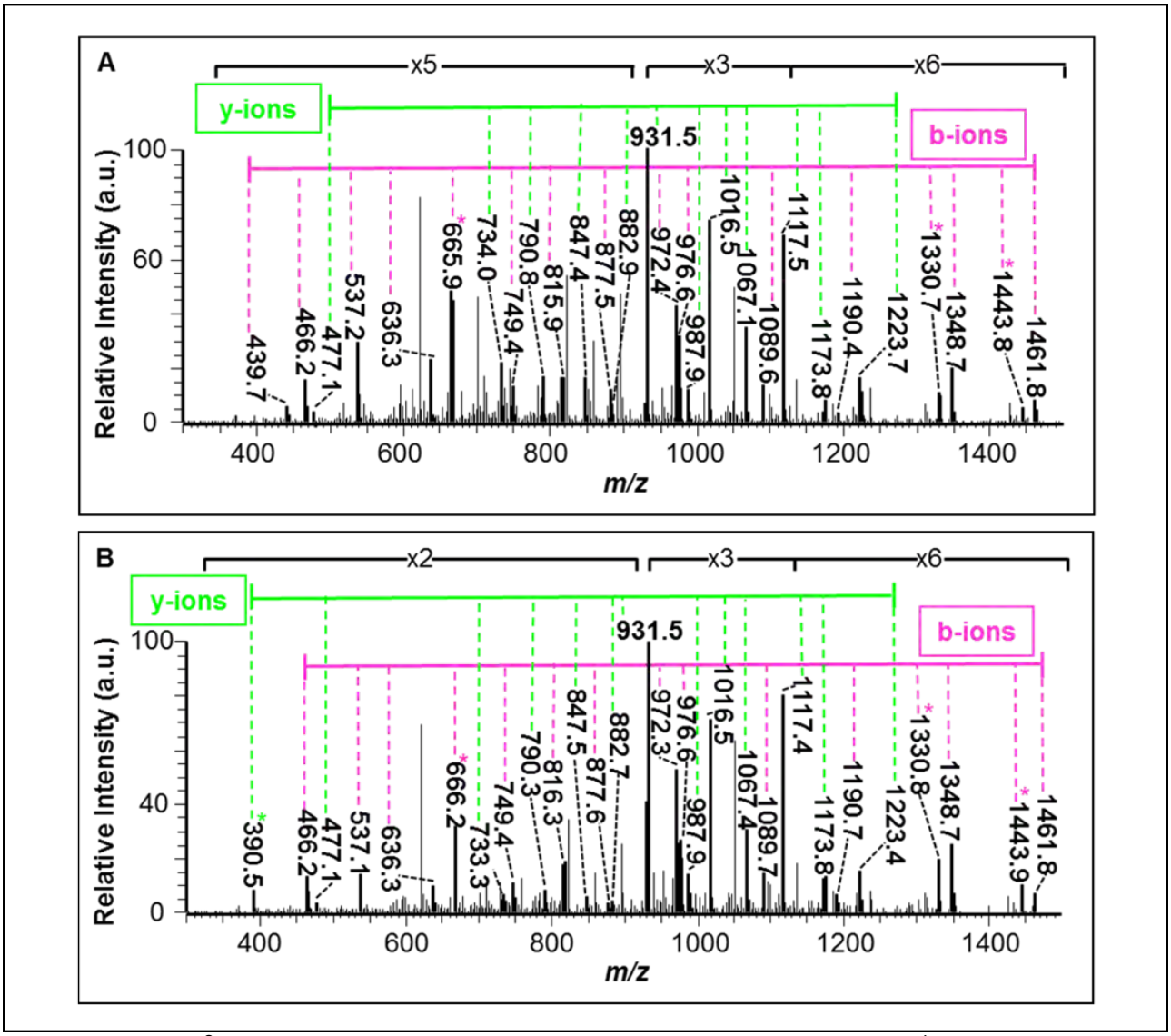


**Fig. S8**. LC-MS$^2$ spectra of the precursor ion at *m/z* 832 for $[M_{P+P} + 4H]^{4+}$ at 10.9 min (**A**) and 11.2 min (**B** and C; Fig. S5). The *y*-type and *b*-type ions are shown on each spectrum. The peaks labelled with an asterisk represent: *m/z* 390.5, $[(y4 - NH_3) + 2H]^{2+}$; *m/z* 665.9, $[(b12_P - H_2O) + 2H]^{2+}$; *m/z* 1330.7, $[(b12_P - H_2O) + H]^{+}$ ; *m/z* 1443.8, $[(b13_P - H_2O) + H]^{+}$. Data are tabulated in Tables S10 and S11.

## 5. Doubly Acylated (2 × Oleoyl) Melittin

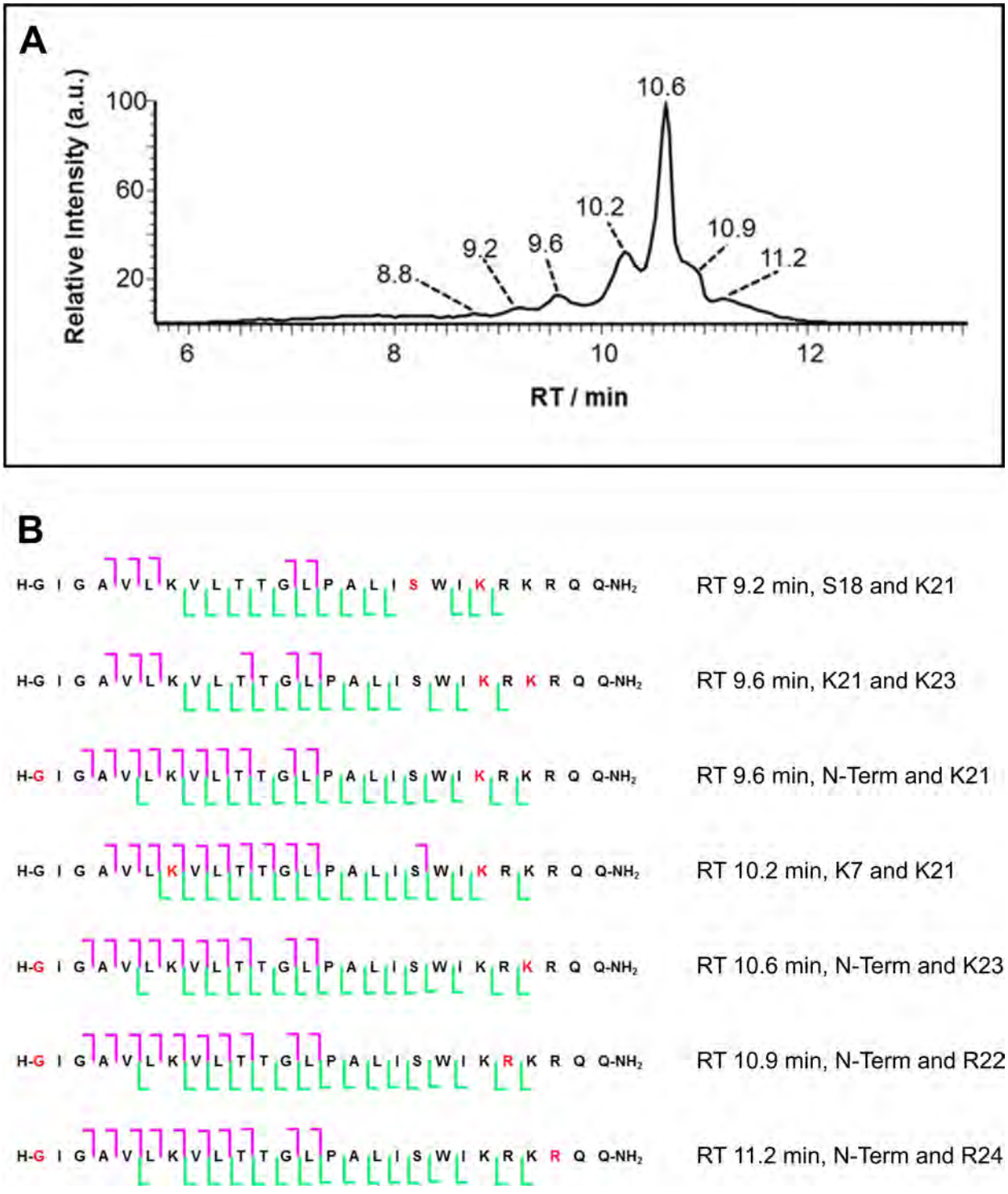


**Fig. S9**. **A**. TIC from CID fragmentation of melittin modified by two oleoyl groups at *m*/*z* 845 (*z* = 4) on ESI-LTQ-MS (LTQFT). Modified melittin was prepared by incubation of synthetic melittin with 50:50 PPC:DOPC over 168 h at 37 °C. **B**. Sequence ladders summarising *y*-type (green) and *b*-type (magenta) ions observed following fragmentation of double oleoylated precursor ions of *m*/*z* 845 (*z* = 4) by CID (LTQ). Acylation sites are highlighted in red. Full details are provided in Figs. S10-S12 and Tables S12-S18.

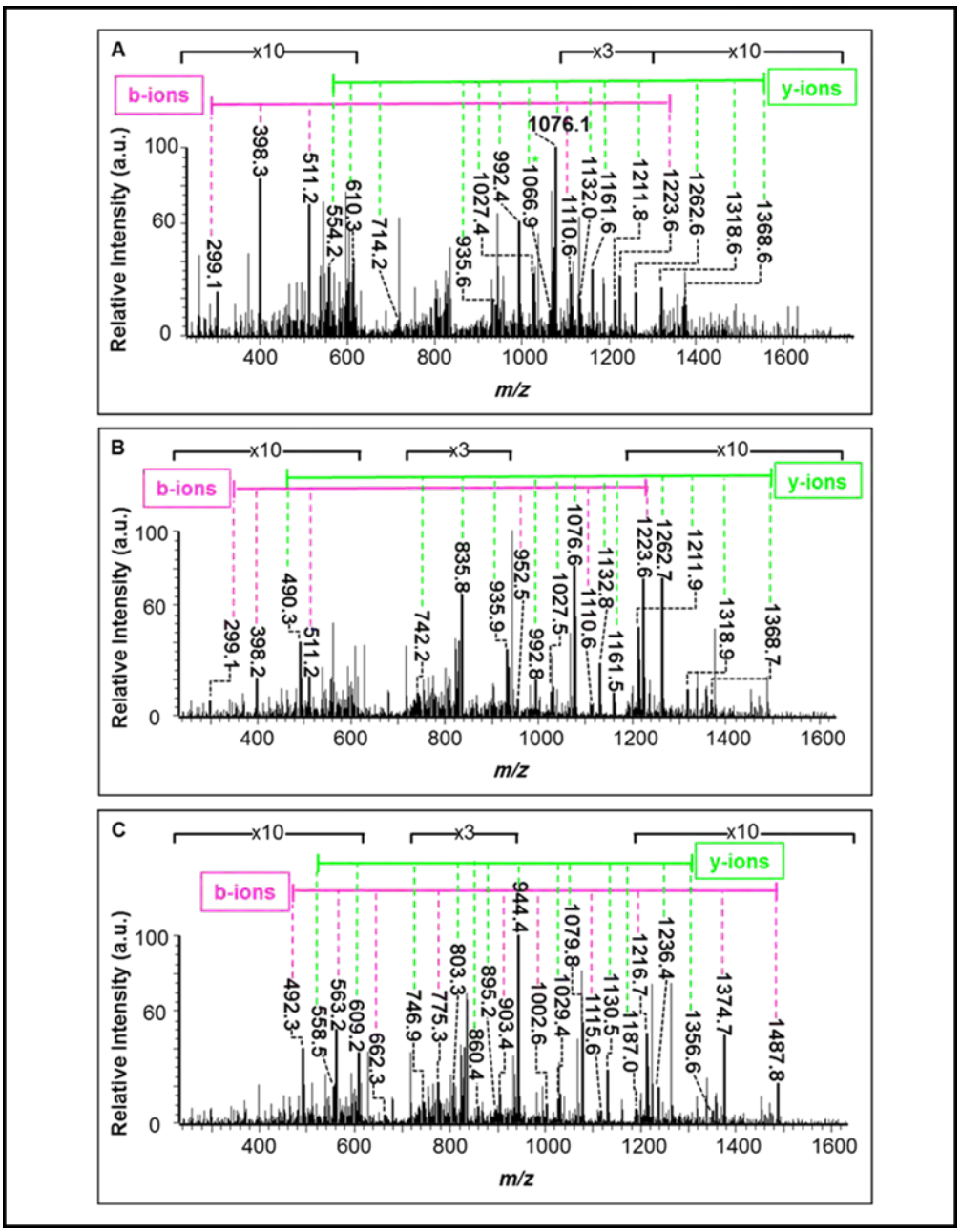


**Fig. S10**. LC-MS$^2$ spectra of the precursor ion at *m/z* 845 for $[M_{O+O} + 4H]^{4+}$ at 9.2 min (**A**) and 9.6 min (**B** and **C**; Fig. S9). The *y*-type and *b*-type ions are shown on each spectrum. The peak labelled with an asterisk in A represents: *m/z* 1066.9, $[(y13_{O+O} + H_2O) – H_2O + 2H]^{2+}$. Data are tabulated in Tables S12 to S14.

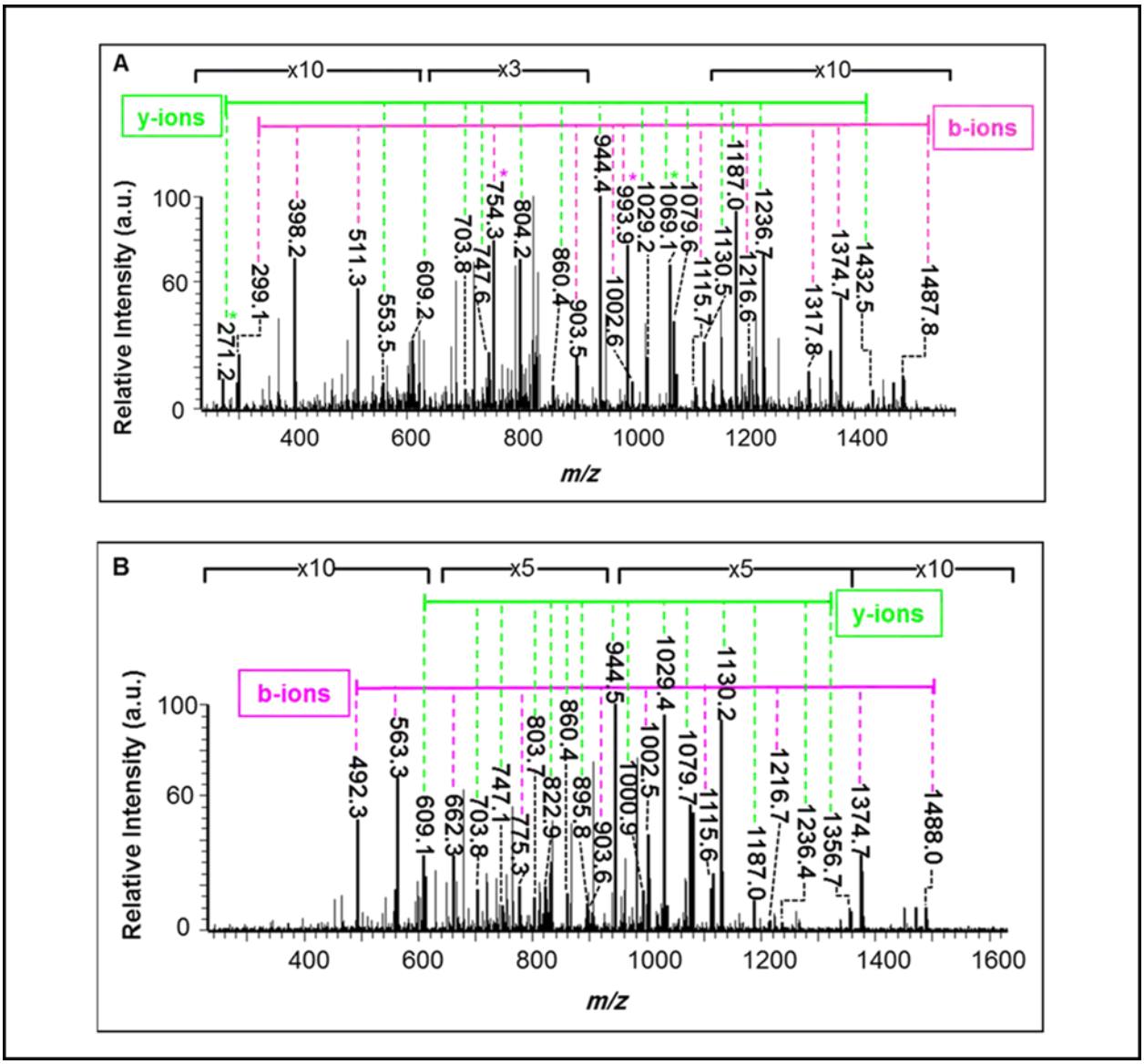


**Fig. S11**. LC-MS$^2$ spectra of the precursor ion at *m/z* 845 for $[M_{O+O} + 4H]^{4+}$ at 10.2 min (**A**) and 10.6 min (**B** and **C**; Fig. S9). The *y*-type and *b*-type ions are shown on each spectrum. The peaks labelled with an asterisk represent: *m/z* 271.2, $[(y4 - NH_3) + 2H]^{2+}$; *m/z* 806.1, $[(y4_O - NH_3) + H]^+$; *m/z* 754.3, $[(b13_O + H_2O) + 2H]^{2+}$; *m/z* 993.9, $[(b18_O + H_2O) + H]^+$; *m/z* 1069.1, $[(y16_O - H_2O) + 2H]^{2+}$. Data are tabulated in Tables S15 and S16.

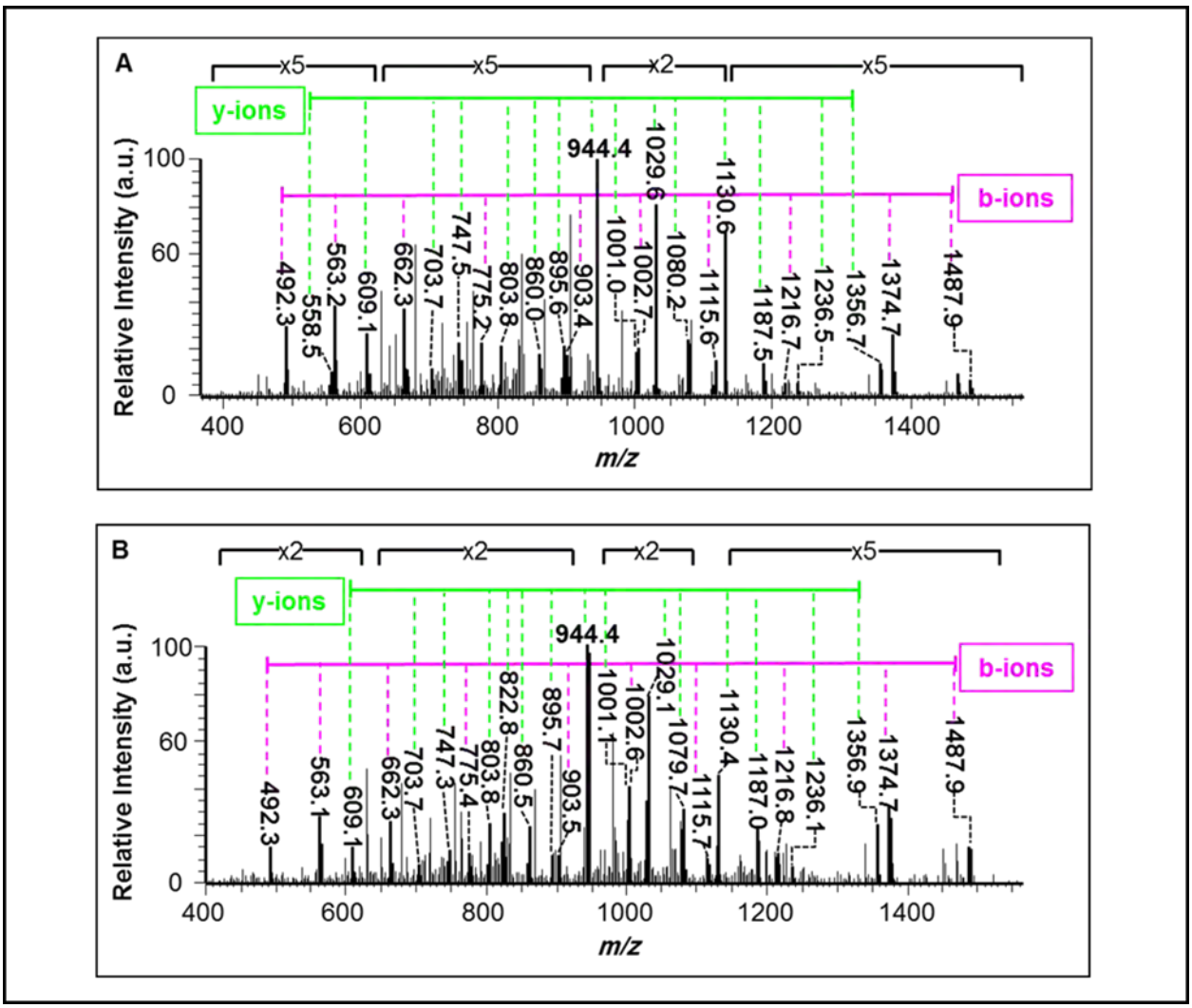


**Fig. S12**. LC-MS$^2$ spectra of the precursor ion at *m/z* 845 for $[M_{O+O} + 4H]^{4+}$ at 10.9 min (**A**) and 11.2 min (**B** and **C**; Fig. S9). The *y*-type and *b*-type ions are shown on each spectrum. Data are tabulated in Tables S17 and S18.

## 6. Doubly Acylated (1 × Oleoyl + 1 × Palmitoyl) Melittin

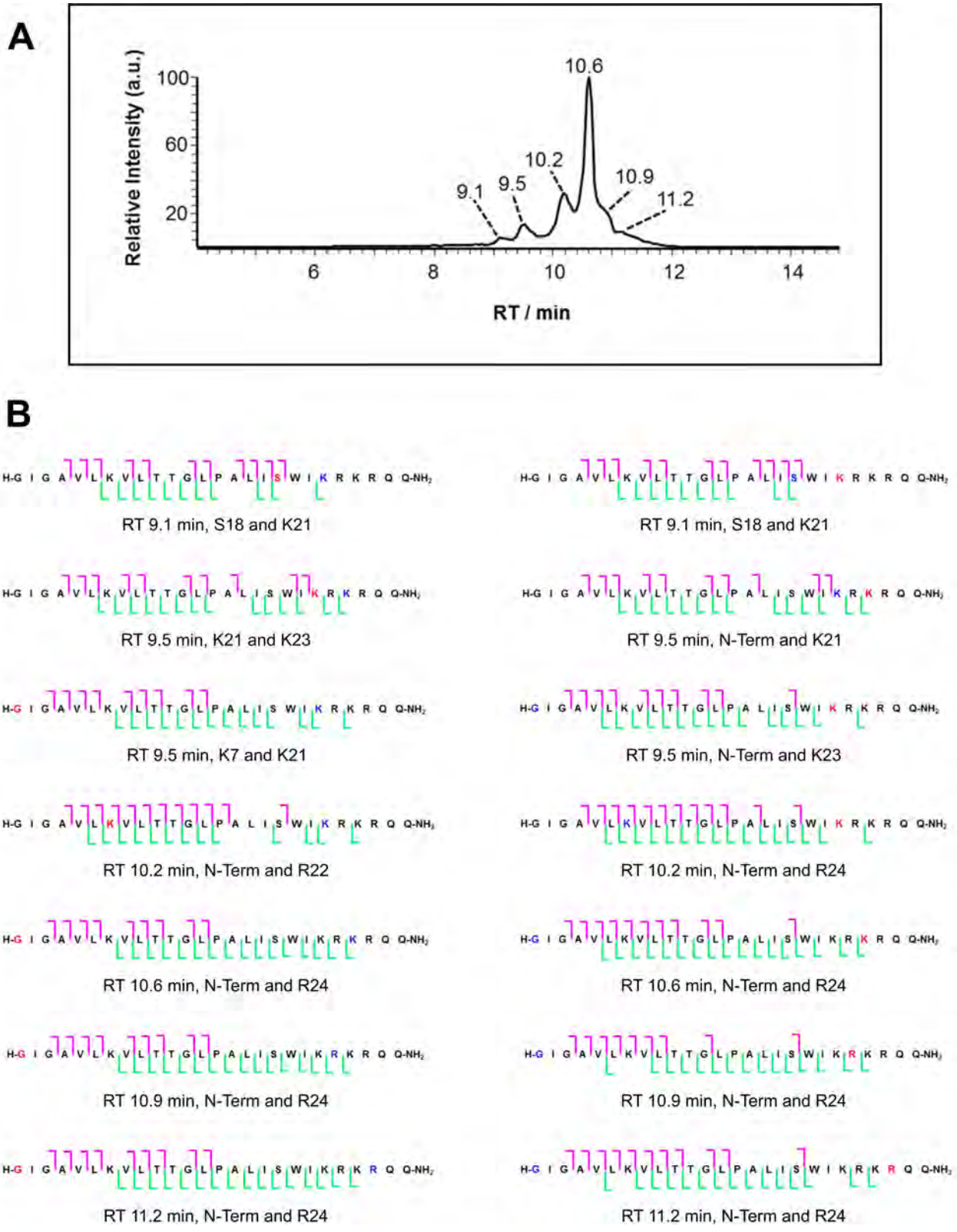


**Fig. S13**. **A**. TIC from CID fragmentation of melittin modified by one palmitoyl and one oleoyl group at *m*/*z* 838 (*z* = 4) on ESI-LTQ-MS (LTQFT). Modified melittin was prepared by incubation of synthetic melittin with 50:50 PPC:DOPC over 168 h at 37 °C. **B**. Sequence ladders summarising *y*-type (green) and *b*-type (magenta) ions observed following fragmentation of double acylated precursor ions of *m*/*z* 838 (*z* = 4) by CID (LTQ). Oleoylation sites are highlighted in red (oleoyl) or blue (palmitoyl). Full details are provided in Figs. S14-S19 and Tables S19-S32.

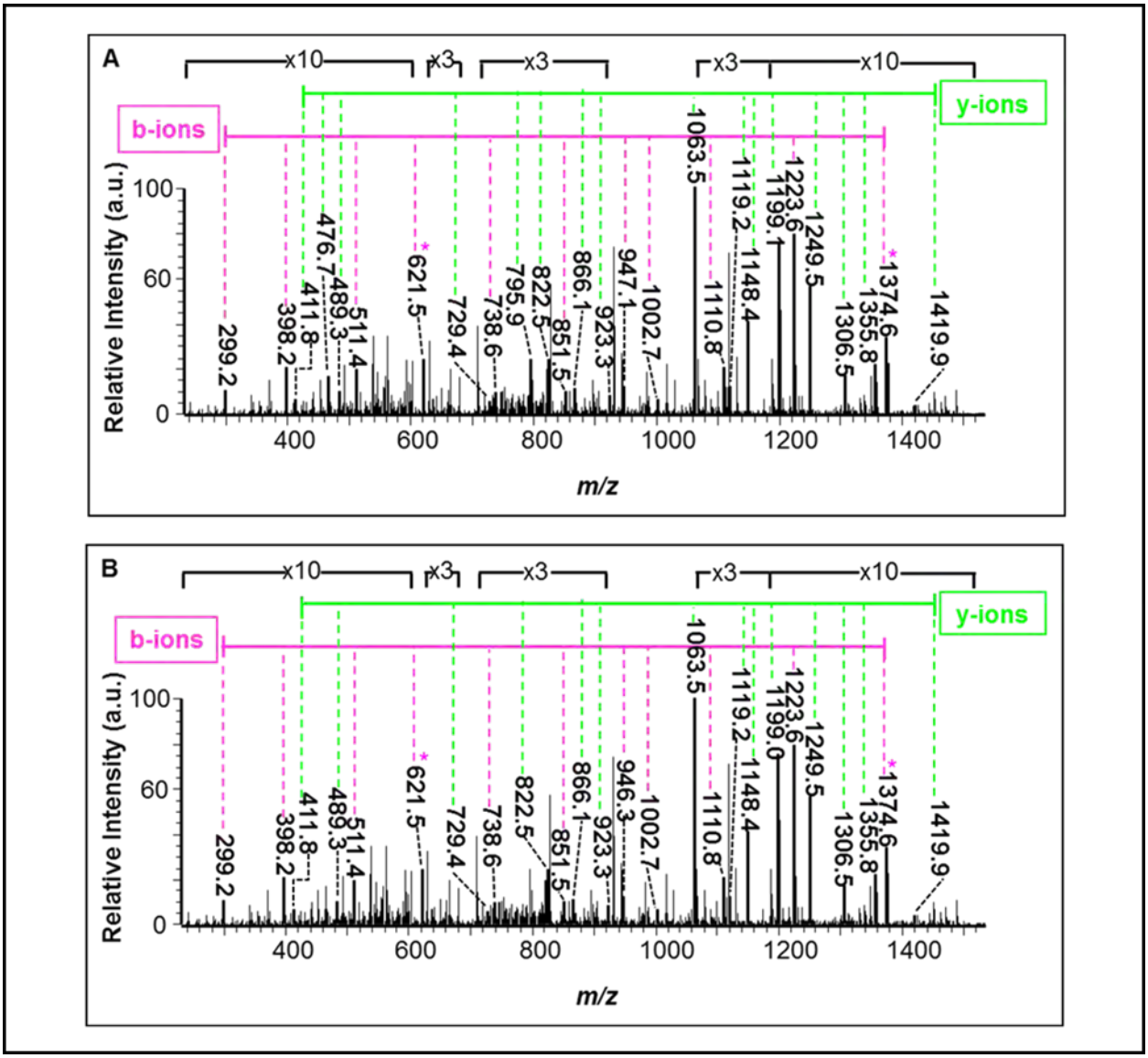


**Fig. S14**. LC-MS$^2$ spectra of the precursor ion at *m/z* 838 for $[M_{P+O} + 4H]^{4+}$ at 9.1 min (Fig. S13). (**A**) corresponds to oleoylation at S18 and palmitoylation at K21. (**B**) corresponds to oleoylation at K21 and palmitoylation at S18. The *y*-type and *b*-type ions are shown on each spectrum. The peaks labelled with an asterisk represent: *m/z* 621.4, $[(b13 + H_2O) + 2H]^{2+}$; *m/z* 1374.6, $[(b15 – NH_3) + H]^{+}$. Data are tabulated in Tables S19 and S20.

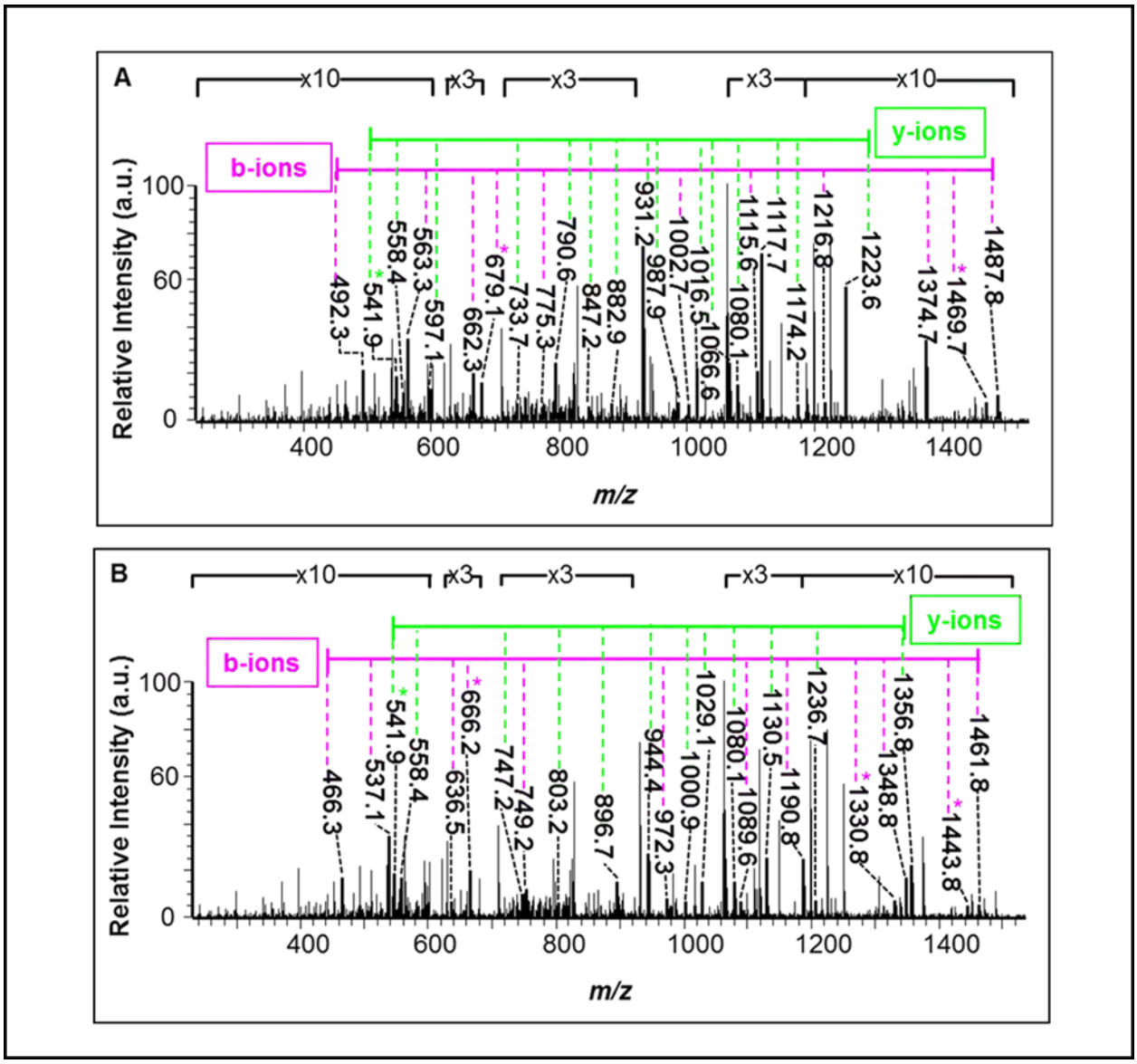


**Fig. S15**. LC-MS$^2$ spectra of the precursor ion at *m/z* 838 for $[M_{P+O} + 4H]^{4+}$ at 9.5 min (Fig. S13). (**A**) corresponds to oleoylation at K21 and palmitoylation at K23. (**B**) corresponds to oleoylation at K23 and palmitoylation at K21. The *y*-type and *b*-type ions are shown on each spectrum. The peaks labelled with an asterisk represent: *m/z* 621.5, $[(b13 + H_2O) + 2H]^{2+}$; *m/z* 1374.6, $[(b15 – NH_3) + H]^+$. Data are tabulated in Tables S21 and S22.

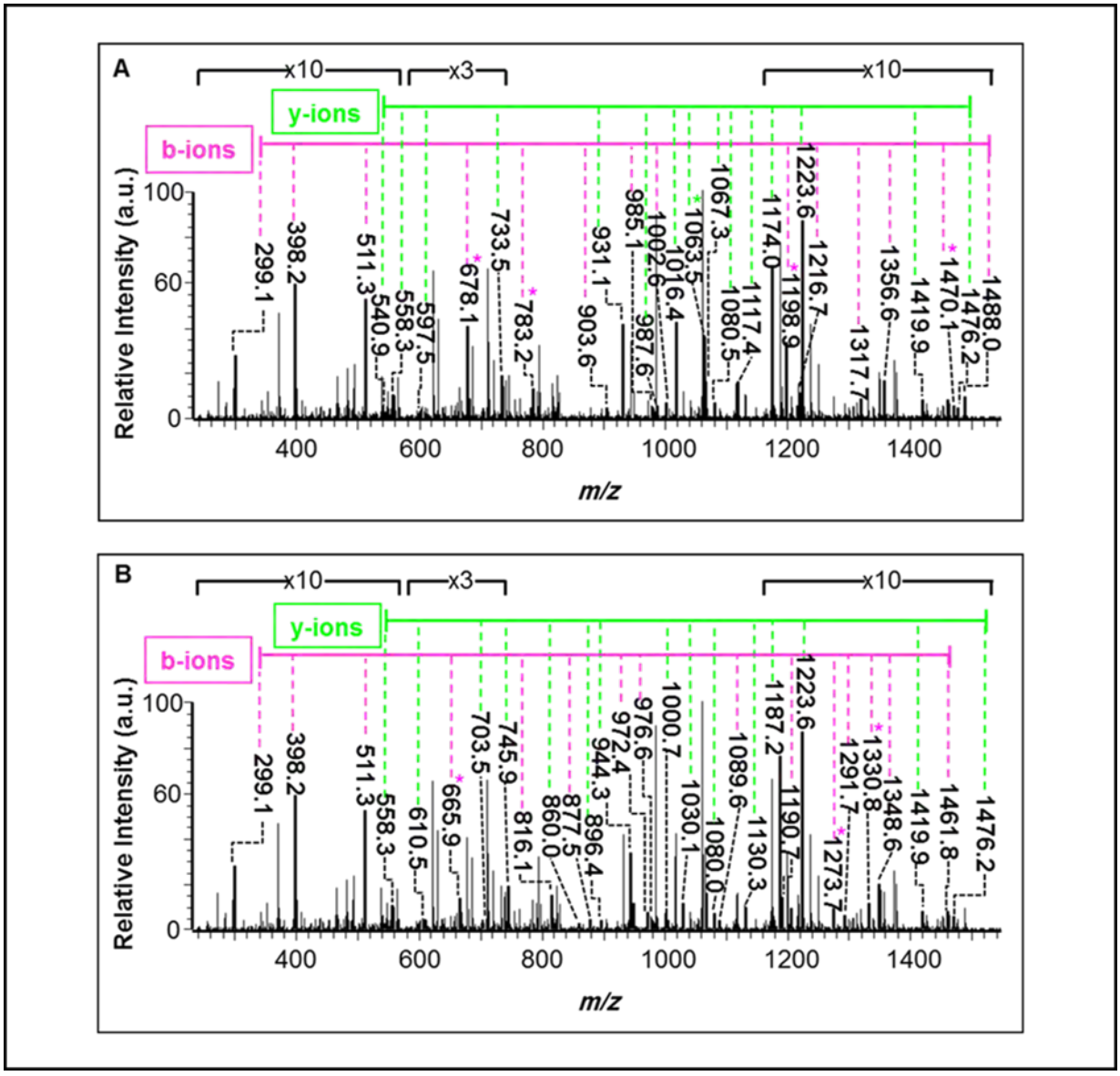


**Fig. S16**. LC-MS$^2$ spectra of the precursor ion at *m/z* 838 for $[M_{P+O} + 4H]^{4+}$ at 10.2 min (Fig. S13). (**A**) corresponds to oleoylation at K7 and palmitoylation at K21. (**B**) corresponds to oleoylation at K21 and palmitoylation at K7. The *y*-type and *b*-type ions are shown on each spectrum. The peaks labelled with an asterisk represent: *m/z* 1198.9, $[(b10_O - H_2O) + H]^+$; *m/z* 1356.6, $[(b12_O - H_2O) + H]^+$; *m/z* 678.1, $[(b12_O - H_2O) + 2H]^{2+}$; *m/z* 1470.1, $[(b13_O - H_2O) + H]^+$; *m/z* 783.2, $[(b14_O - H_2O) + H]^{2+}$; *m/z* 1273.7, $[(b11_P - H_2O) + H]^+$; *m/z* 1330.8, $[(b12_P - H_2O) + H]^+$; *m/z* 665.9, $[(b12_P - H_2O) + 2H]^{2+}$; *m/z* 1063.5, $[(y6_O - NH_3) + H]^+$. Data are tabulated in Tables S25 and S26.

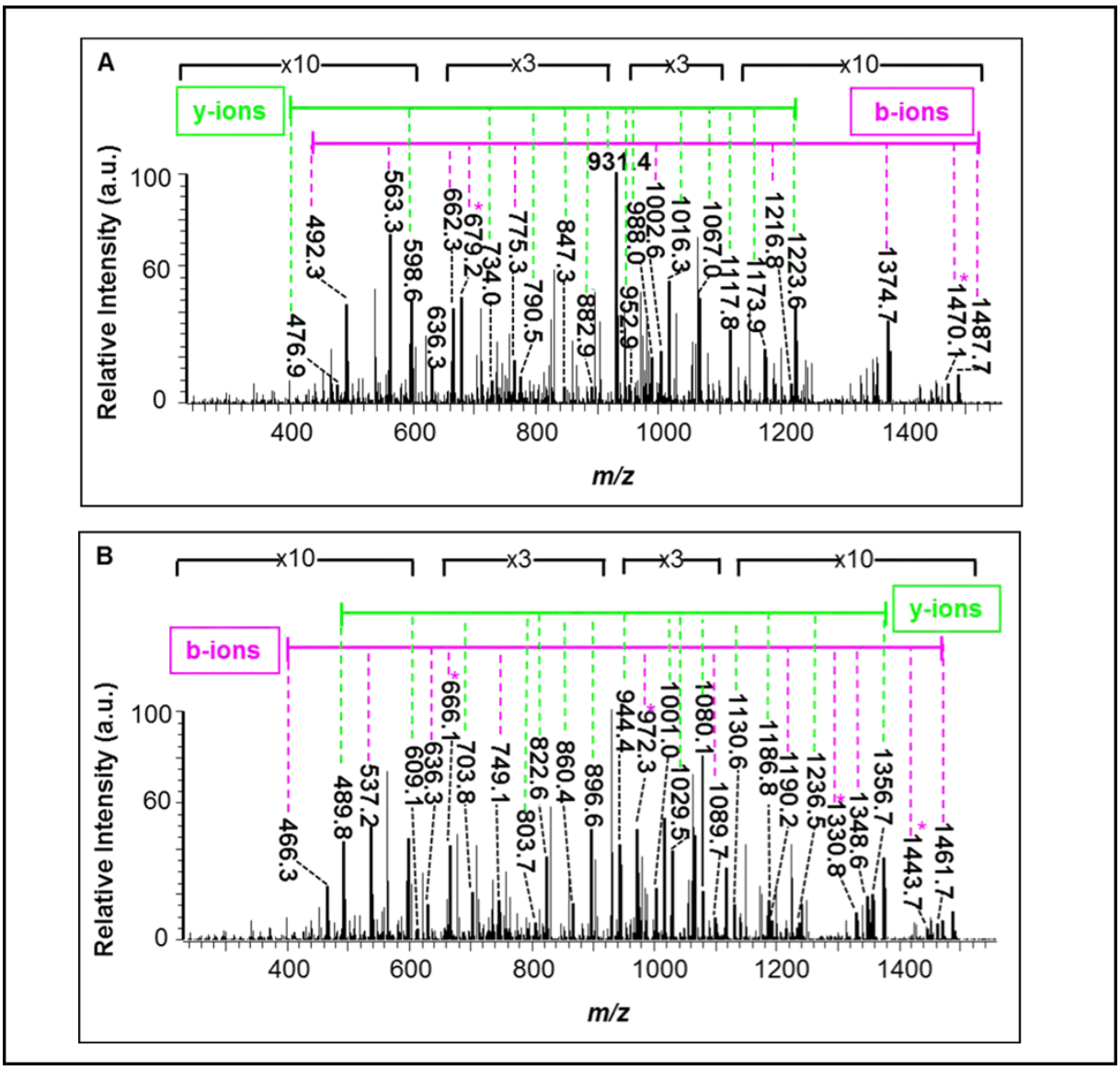


**Fig. S17**. LC-MS$^2$ spectra of the precursor ion at *m/z* 838 for $[M_{P+O} + 4H]^{4+}$ at 10.6 min (Fig. S13). (**A**) corresponds to oleoylation at the *N*-terminus and palmitoylation at K23. (**B**) corresponds to oleoylation at K23 and palmitoylation at the *N*-terminus. The *y*-type and *b*-type ions are shown on each spectrum. The peaks labelled with an asterisk represent: *m/z* 679.2, $[(b5_O + H_2O) + H]^+$; *m/z* 1470.1, $[(b13_O – H_2O) + H]^+$; *m/z* 1330.8, $[(b12_P – H_2O) + H]^+$; *m/z* 666.1, $[(b12_P – H_2O) + 2H]^{2+}$; *m/z* 1443.7, $[(b13_P – H_2O) + H]^+$; *m/z* 779.7, $[(y4_P – NH_3) + H]^+$. Data are tabulated in Tables S27 and S28.

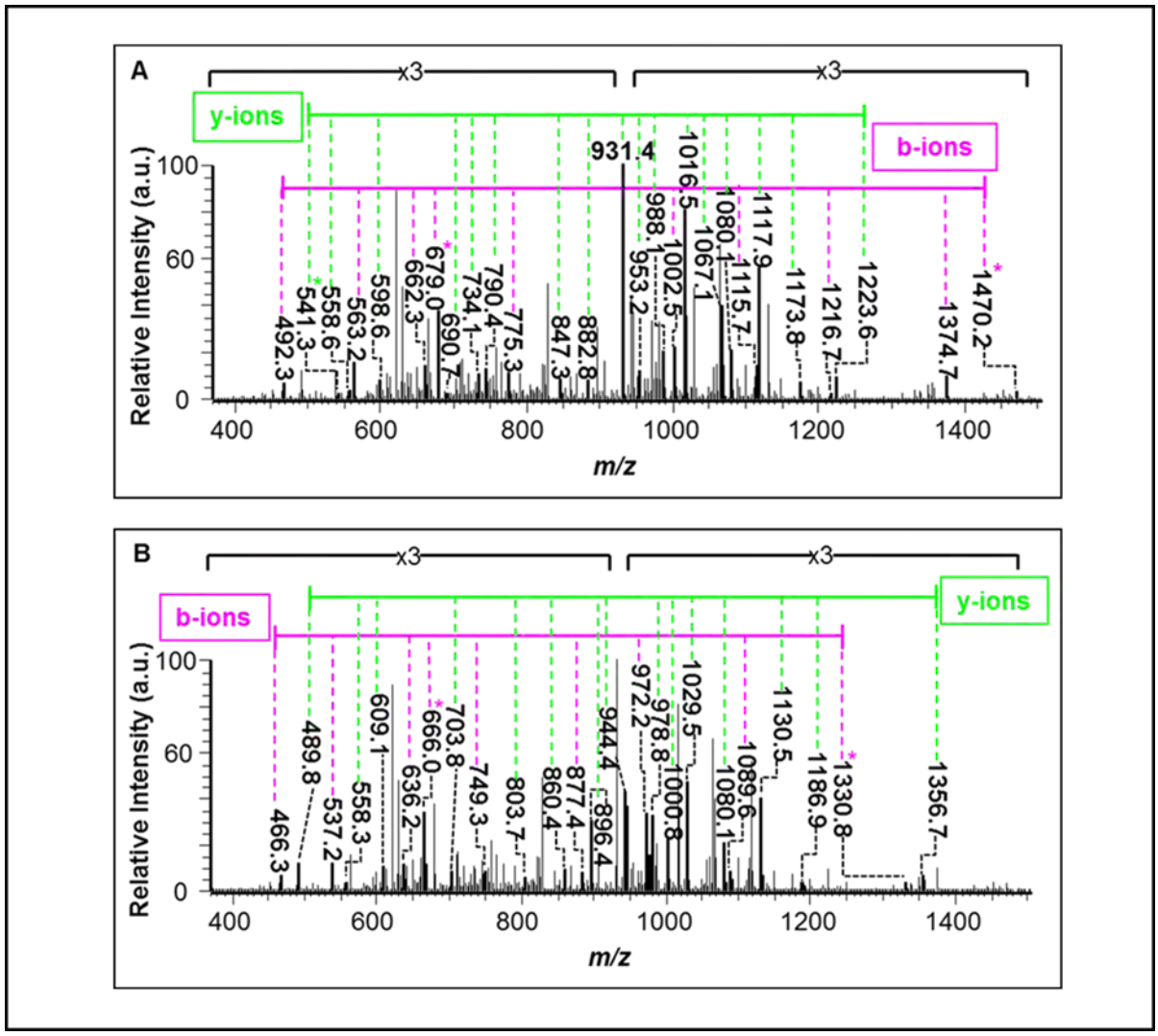


**Fig. S18**. LC-MS$^2$ spectra of the precursor ion at *m/z* 838 for $[M_{P+O} + 4H]^{4+}$ at 10.9 min (Fig. S13). (**A**) corresponds to oleoylation at the *N*-terminus and palmitoylation at R22. (**B**) corresponds to oleoylation at R22 and palmitoylation at the *N*-terminus. The *y*-type and *b*-type ions are shown on each spectrum. The peaks labelled with an asterisk represent: *m/z* 679.0, $[(b5_O + H_2O) + H]^+$; *m/z* 1470.2, $[(b13_O – H_2O) + H]^+$; *m/z* 1330.8, $[(b12_P – H_2O) + H]^+$; *m/z* 666.0, $[(b12_P – H_2O) + 2H]^{2+}$; *m/z* 541.3, $[(y4 – NH_3) + H]^+$. Data are tabulated in Tables S29 and S30.

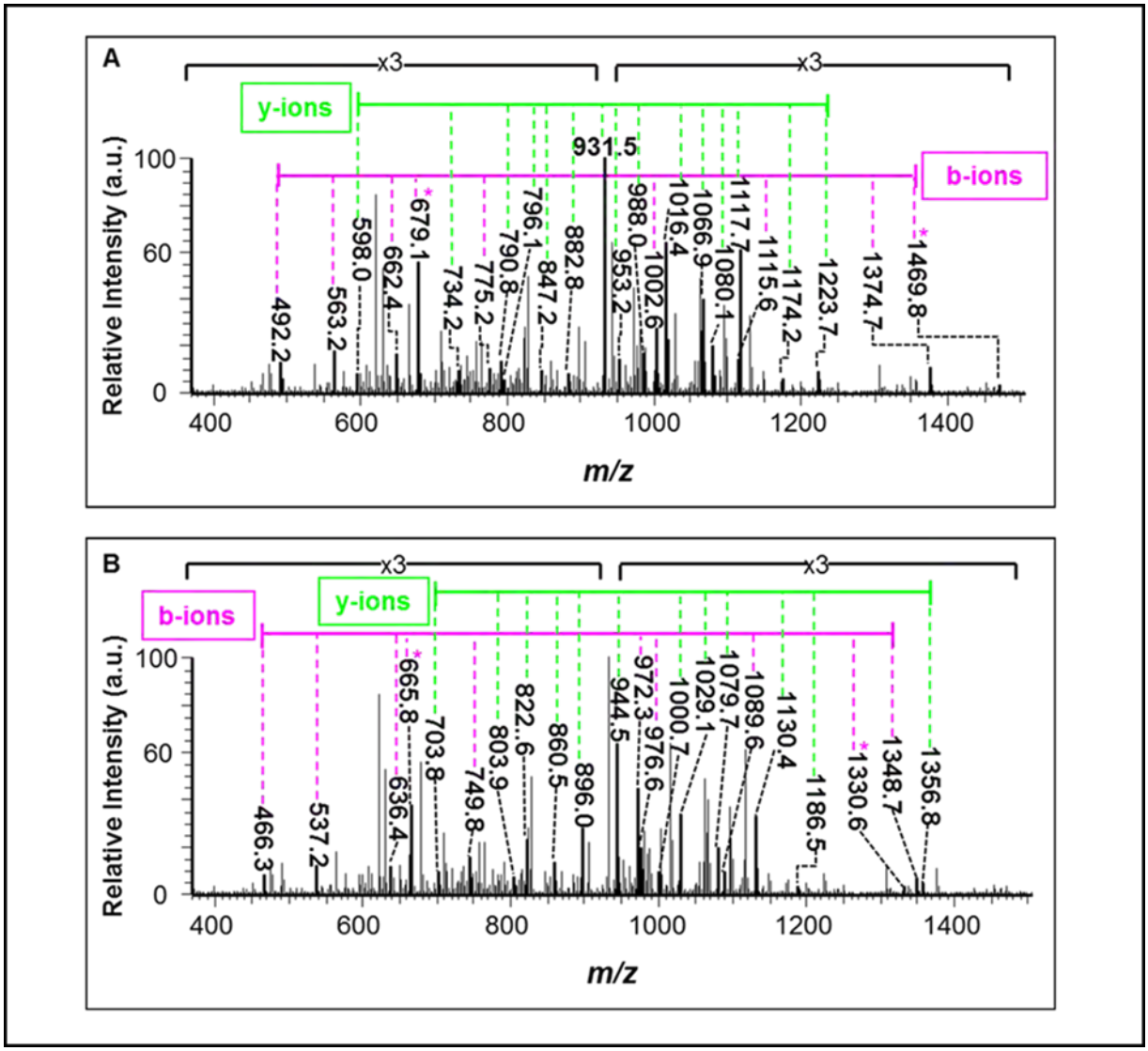


**Fig. S19**. LC-MS$^2$ spectra of the precursor ion at *m/z* 838 for $[M_{P+O} + 4H]^{4+}$ at 11.2 min (Fig. S13). (**A**) corresponds to oleoylation at the *N*-terminus and palmitoylation at R24. (**B**) corresponds to oleoylation at R24 and palmitoylation at the *N*-terminus. The *y*-type and *b*-type ions are shown on each spectrum. The labelled peak with the asterisk represent: *m/z* 679.1, $[(b5_O + H_2O) + H]^+$; *m/z* 1469.8, $[(b13_P – H_2O) + H]^+$; *m/z* 1330.8, $[(b12_P – H_2O) + H]^+$; *m/z* 665.8, $[(b12_P – H_2O) + 2H]^{2+}$; *m/z* 779.5, $[(y4_P – NH_3) + H]^+$. Data are tabulated in Tables S31 and S32.

**Supporting Information: Other Figures**

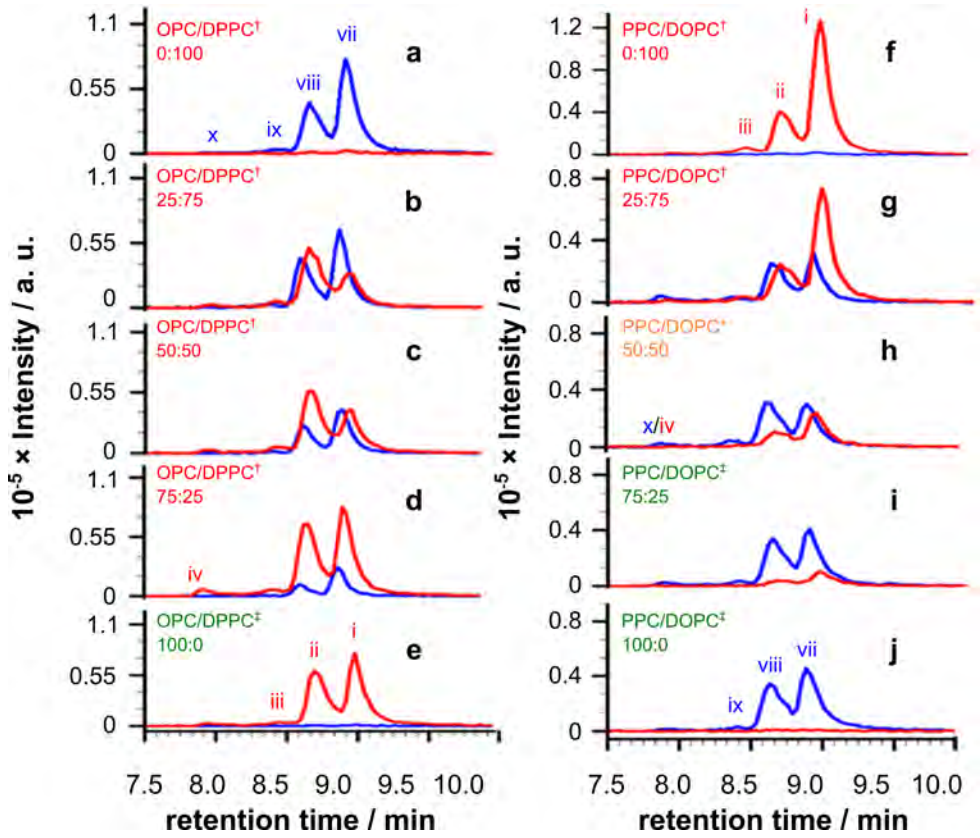


**Fig. S20**. EICs for *m/z* 772.00 and 778.51, corresponding to palmitoyl and oleoyl melittin respectively (*z* = 4), from LC-MS analyses of synthetic melittin incubated for 48 h with mixtures of lysolipid and lipid at 37 °C in buffer (10 mM $NaHCO_3$/90 mM NaCl) at pH 7.4. a) to e) DPPC + OPC; f) to j) DOPC + PPC. The initial molar ratio of lysolipid to lipid is indicated on each trace. Ratios indicated with a dagger (†) are bilayer ± lysolipid; those indicated with an asterisk (*) are mixed bilayer/detergent systems; those indicated with a double dagger (‡) are micelles (on the basis of literature precedents).[1–4] Peak annotations are identified in Figs. 2 and 3 in the main article.

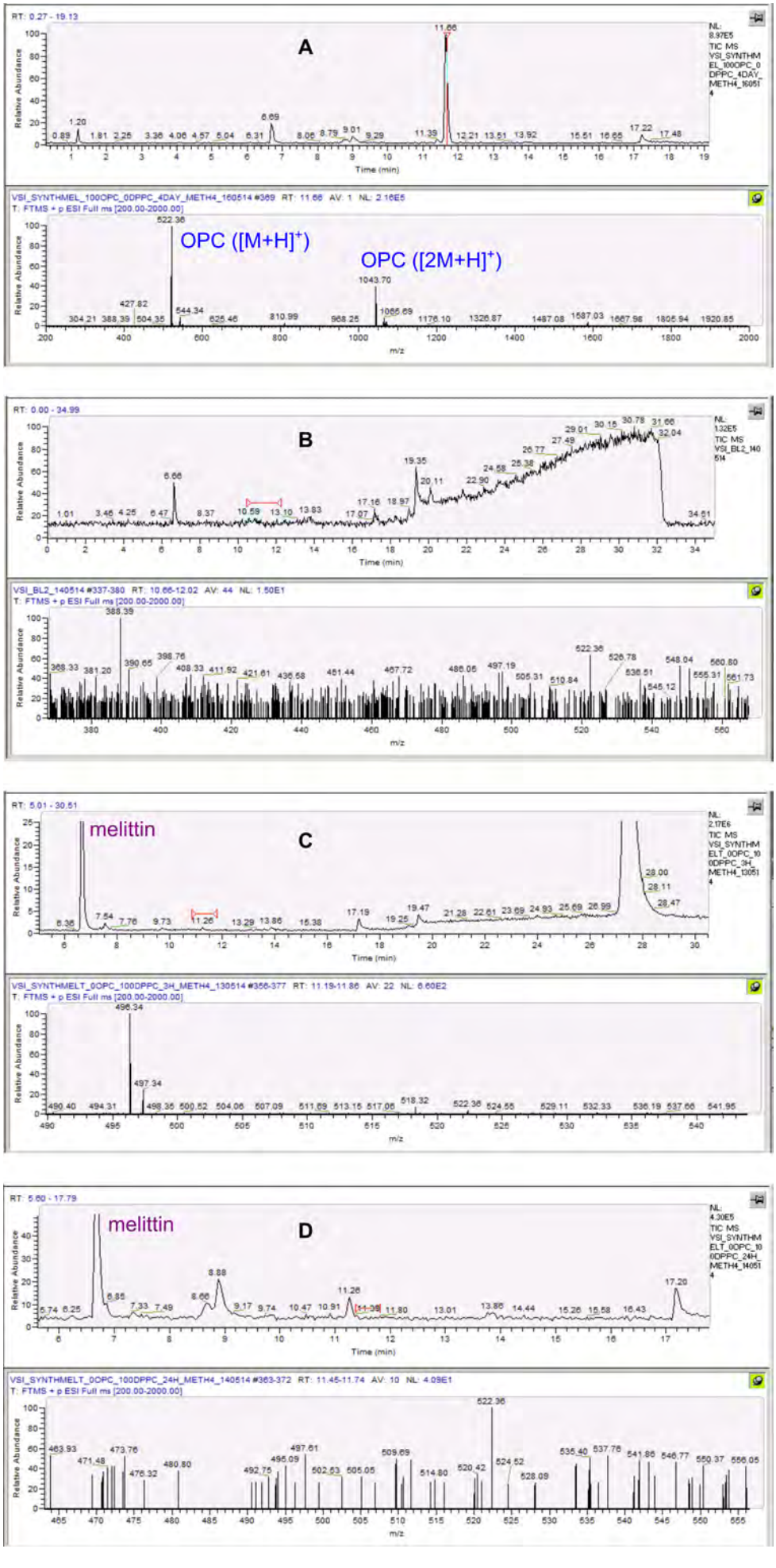


**Fig. S21**. LC-MS analyses for authentic OPC, and mixtures of DPPC liposomes with melittin. **A** is an authentic sample of OPC; **B** is a blank run; **C** is 3 h following the addition of melittin to DPPC; **D** is 24 h after the addition of DPPC to melittin. Both **C** and **D** show the presence of OPC at levels higher than the blank run, suggesting a small amount of OPC contamination in the sample.

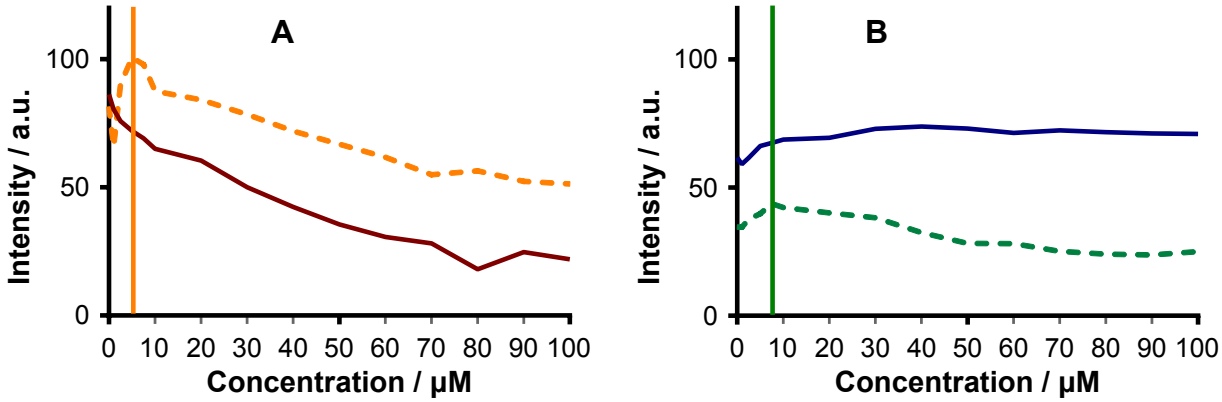


**Fig. S22**. Rhodamine 6G emission at 550 nm in the presence of increasing concentrations of lipidated melittin (1–100 μM) in water. **A**. *N*-palmitoyl melittin (solid red); K23-palmitoyl melittin (dashed orange). The vertical line denotes the CMC of K23-palmitoyl melittin at approximately 5 μm. **B**. *N*-oleoyl melittin (solid blue); K23-oleoyl melittin (dashed green). The vertical line indicates the CMC of K23-oleoyl melittin at approximately 7.5 μm.

# Supporting Information: Tables

## Table S1. Oleoylated melittin species observed in a mixture of melittin and OPC incubated at 37 °C over 168 h.

| $^{1}$H-GIGAVLKVLTTGLPALISWIKRKRQQ-$NH_2^{26}$ | | | | | | |
|---|---|---|---|---|---|---|
| *m/z* Theor‡ | *m/z* Meas‡ | *z* | RT (min) | Error (ppm) | Peak Area / $10^5$ (a.u. min)§ | Assignment |
| 1037.3404 | 1037.3416 | 3 | 8.6 | 1.16 | 121 ± 79 | [1-26] + 1 × (C18:1) / Single Oleoylation |
| 778.2572 | 778.2581 | 4 | 8.6 | 1.16 | 422 ± 268 | [1-26] + 1 × (C18:1) / Single Oleoylation |
| 622.8072 | 622.8076 | 5 | 8.6 | 0.64 | 355 ± 229 | [1-26] + 1 × (C18:1) / Single Oleoylation |
| 1125.4222 | 1125.4241 | 3 | 11.1 | 1.69 | 93 ± 76 | [1-26] + 2 × (C18:1) / Double Oleoylation |
| 844.3185 | 844.3196 | 4 | 11.1 | 1.30 | 432 ± 346 | [1-26] + 2 × (C18:1) / Double Oleoylation |
| 675.6562 | 675.6574 | 5 | 11.2 | 1.78 | 46 ± 35 | [1-26] + 2 × (C18:1) / Double Oleoylation |
| 1125.4222 | 1125.4231 | 3 | 17.8 | 0.80 | 0.7 ± 0.2 | [1-26] + 2 × (C18:1) / Labile Triple Oleoylation |
| 844.3185 | 844.3192 | 4 | 17.8 | 0.83 | 6 ± 2 | [1-26] + 2 × (C18:1) / Labile Triple Oleoylation |
| 675.6562 | 675.6555 | 5 | 17.8 | -1.04 | 0.4 ± 0.1 | [1-26] + 2 × (C18:1) / Labile Triple Oleoylation |
| 1213.5040 | 1213.5055 | 3 | 18.2 | 1.24 | 0.5 ± 0.3 | [1-26] + 3 × (C18:1) / Triple Oleoylation |
| 910.3798 | 910.3790 | 4 | 18.2 | -0.90 | 1.5 ± 0.5 | [1-26] + 3 × (C18:1) / Triple Oleoylation |

‡ Both theoretical (Theor) and measured (Meas) *m/z* values are for the monoisotopic peak. Theoretical masses were obtained from mMass software (V5.5).

§ Errors are reported as the standard error of the mean (SEM) of the peak area (A), *n*=3.

## Table S2. Palmitoylated melittin species observed in a mixture of melittin and PPC incubated at 37 °C over 168 h.

| $^{1}$H-GIGAVLKVLTTGLPALISWIKRKRQQ-$NH_2^{26}$ | | | | | | |
|---|---|---|---|---|---|---|
| *m/z* Theor‡ | *m/z* Meas‡ | *z* | RT (min) | Error (ppm) | Peak Area / $10^5$ (a.u. min)§ | Assignment |
| 1028.6686 | 1028.6675 | 3 | 8.8 | -1.07 | 43 ± 42 | [1-26] + 1 × (C16:0) / Single Palmitoylation |
| 771.7532 | 771.7540 | 4 | 8.9 | 1.04 | 102 ± 96 | [1-26] + 1 × (C16:0) / Single Palmitoylation |
| 617.6040 | 617.6046 | 5 | 8.9 | 0.97 | 59 ± 55 | [1-26] + 1 × (C16:0) /Single Palmitoylation |
| 1108.0784 | 1108.0837 | 3 | 11.3 | 4.78 | 0.1 ± 0.04 | [1-26] + 2 × (C16:0) / Double Palmitoylation |
| 831.3107 | 831.3134 | 4 | 11.2 | 3.25 | 0.7 ± 0.1 | [1-26] + 2 × (C16:0) / Double Palmitoylation |
| 1108.0784 | 1108.0756 | 3 | 17.7 | -2.52 | 0.1 ± 0.1 | [1-26] + 2 × (C16:0) / Labile Triple Palmitoylation |
| 831.3107 | 831.3109 | 4 | 17.7 | 0.24 | 1 ± 0.7 | [1-26] + 2 × (C16:0) / Labile Triple Palmitoylation |

‡ Both theoretical and measured *m/z* values are for monoisotopic peak. Theoretical mass obtained from mMass software (V5.5).

§ Errors are reported as SEM of peak area (*n*=2).

**Table S3. Acylated species observed in a mixture of melittin with PPC:DOPC (1:1) after incubation at 37 °C for 168 h.**

| $^{1}$H-GIGAVLKVLTTGLPALISWIKRKRQQ-$NH_2^{26}$ | | | | | | |
|---|---|---|---|---|---|---|
| *m/z* Theor‡ | *m/z* Meas‡ | *z* | RT (min) | Error (ppm) | Peak Area / $10^4$ (a.u. min)§ | Assignment |
| 1037.3404 | 1037.3423 | 3 | 8.9 | 1.83 | 55 ± 16 | [1-26] + 1 × (C18:1) / Single Oleoylation |
| 778.2572 | 778.2580 | 4 | 8.9 | 1.03 | 266 ± 57 | [1-26] + 1 × (C18:1) / Single Oleoylation |
| 622.8072 | 622.8076 | 5 | 8.9 | 0.64 | 137 ± 121 | [1-26] + 1 × (C18:1) / Single Oleoylation |
| 1028.6686 | 1028.6689 | 3 | 8.5 | 0.29 | 63 ± 22 | [1-26] + 1 × (C16:0) / Single Palmitoylation |
| 771.7532 | 771.7532 | 4 | 8.5 | 0.00 | 260 ± 42 | [1-26] + 1 × (C16:0) / Single Palmitoylation |
| 617.6040 | 617.6048 | 5 | 8.5 | 1.30 | 238 ± 56 | [1-26] + 1 × (C16:0) /Single Palmitoylation |
| 1125.4222 | 1125.4205 | 3 | 11.0 | -1.51 | 31 ± 15 | [1-26] + 2 × (C18:1) / Double Oleoylation |
| 844.3185 | 844.3196 | 4 | 11.0 | 1.30 | 129 ± 37 | [1-26] + 2 × (C18:1) / Double Oleoylation |
| 675.6562 | 675.6562 | 5 | 10.9 | 0.00 | 21 ± 6 | [1-26] + 2 × (C18:1) / Double Oleoylation |
| 1108.0784 | 1108.0811 | 3 | 11.0 | 2.44 | 46 ± 17 | [1-26] + 2 × (C16:0) / Double Palmitoylation |
| 831.3107 | 831.3117 | 4 | 10.9 | 1.20 | 168 ± 48 | [1-26] + 2 × (C16:0) / Double Palmitoylation |
| 665.2500 | 665.2509 | 5 | 10.9 | 1.35 | 38 ± 8 | [1-26] + 2 × (C16:0) / Double Palmitoylation |
| 1116.7503 | 1116.7489 | 3 | 11.0 | -1.25 | 78 ± 29 | [1-26] + 1 × (C16:0) + 1 × (C18:1)/ Palmitoylation + Oleoylation |
| 837.8146 | 837.8157 | 4 | 10.9 | 1.31 | 273 ± 62 | [1-26] + 1 × (C16:0) + 1 × (C18:1)/ Palmitoylation + Oleoylation |
| 670.4531 | 670.4540 | 5 | 10.8 | 1.34 | 67 ± 19 | [1-26] + 1 × (C16:0) + 1 × (C18:1)/ Palmitoylation + Oleoylation |
| 1125.4222 | 1125.4242 | 3 | 17.8 | 1.78 | 0.3 ± 0.2 | [1-26] + 2 × (C18:1) + / Labile Triple Oleoylation |
| 844.3185 | 844.3190 | 4 | 17.8 | 0.59 | 5 ± 4 | [1-26] + 2 × (C18:1) + / Labile Triple Oleoylation |
| 1108.0784 | 1108.0554 | 3 | 17.7 | -20.76 | 1 ± 0.4 | [1-26] + 2 × (C16:0) + / Labile Triple Palmitoylation |
| 831.3107 | 831.3108 | 4 | 17.8 | 0.12 | 6 ± 5 | [1-26] + 2 × (C16:0) + / Labile Triple Palmitoylation |
| 1116.7503 | 1116.7476 | 3 | 17.7 | -2.42 | 1.5 ± 1 | [1-26] + 1 × (C16:0) + 1 × (C18:1)/ Labile (Palmitoylation + Oleoylation) |
| 837.8146 | 837.8159 | 4 | 17.7 | 1.55 | 12 ± 9 | [1-26] + 1 × (C16:0) + 1 × (C18:1)/ Labile (Palmitoylation + Oleoylation) |
| 670.4531 | 670.4553 | 5 | 17.8 | 3.28 | 0.5 ± 0.2 | [1-26] + 1 × (C16:0) + 1 × (C18:1)/ Labile (Palmitoylation + Oleoylation) |
| 1213.5040 | 1213.5038 | 3 | 18.18 | -0.16 | 1 ± 1 | [1-26] + 3 × (C18:1) / Triple Oleoylation |
| 910.3798 | 910.3758 | 4 | 18.09 | -4.39 | 2 ± 2 | [1-26] + 3 × (C18:1) / Triple Oleoylation |
| 1187.4883 | 1187.4899 | 3 | 18.15 | 1.35 | 1 ± 1 | [1-26] + 3 × (C16:0) / Triple Palmitoylation |
| 890.8681 | 890.8683 | 4 | 18.21 | 0.22 | 4 ± 3 | [1-26] + 3 × (C16:0) / Triple Palmitoylation |
| 1204.8321 | 1204.8300 | 3 | 18.18 | -1.74 | 2.5 ± 2 | [1-26] + 2 × (C18:1) + 1 × (C16:0) / Double Oleoylation + Single Palmitoylation |
| 903.8759 | 903.8759 | 4 | 18.12 | 0.00 | 8 ± 7.5 | [1-26] + 2 × (C18:1) + 1 × (C16:0) / Double Oleoylation + Single Palmitoylation |
| 1196.1602 | 1196.1633 | 3 | 18.18 | 2.59 | 2 ± 2 | [1-26] + 2 × (C16:0) + 1 × (C18:1) / Double Palmitoylation + Single Oleoylation |
| 897.3720 | 897.3736 | 4 | 18.21 | 1.78 | 10 ± 9 | [1-26] + 2 × (C16:0) + 1 × (C18:1) / Double Palmitoylation + Single Oleoylation |

‡ Both theoretical and measured *m/z* values are for the monoisotopic peak. Theoretical mass obtained from mMass software (V5.5).

§ Errors are reported as SEM of peak area (*n*=2).

**Table S4. Acylated species observed in a mixture of melittin with OPC:DPPC (1:1) after incubation at 37 °C for 168 h.**

| $^{1}$H-GIGAVLKVLTTGLPALISWIKRKRQQ-$NH_2^{26}$ | | | | | | |
|---|---|---|---|---|---|---|
| *m/z* Theor‡ | *m/z* Meas‡ | *z* | RT (min) | Error (ppm) | Peak Area / $10^4$ (a.u. min)§ | Assignment |
| 1037.3404 | 1037.3405 | 3 | 8.6 | 0.09 | 144 ± 67 | [1-26] + 1 × (C18:1) / Single Oleoylation |
| 778.2572 | 778.2585 | 4 | 8.6 | 1.67 | 660 ± 307 | [1-26] + 1 × (C18:1) / Single Oleoylation |
| 622.8072 | 622.8077 | 5 | 8.6 | 0.80 | 479 ± 159 | [1-26] + 1 × (C18:1) / Single Oleoylation |
| 1028.6686 | 1028.6687 | 3 | 8.5 | 0.10 | 85 ± 33 | [1-26] + 1 × (C16:0) / Single Palmitoylation |
| 771.7532 | 771.7542 | 4 | 8.5 | 1.30 | 364 ± 102 | [1-26] + 1 × (C16:0) / Single Palmitoylation |
| 617.6040 | 617.6046 | 5 | 8.5 | 0.97 | 270 ± 48 | [1-26] + 1 × (C16:0) /Single Palmitoylation |
| 1125.4222 | 1125.4232 | 3 | 11.0 | 0.89 | 24 ± 15 | [1-26] + 2 × (C18:1) / Double Oleoylation |
| 844.3185 | 844.3193 | 4 | 10.9 | 0.95 | 282 ± 30 | [1-26] + 2 × (C18:1) / Double Oleoylation |
| 675.6562 | 675.6549 | 5 | 10.9 | -1.92 | 35 ± 19 | [1-26] + 2 × (C18:1) / Double Oleoylation |
| 1108.0784 | 1108.0789 | 3 | 11.0 | 0.45 | 19 ± 9 | [1-26] + 2 × (C16:0) / Double Palmitoylation |
| 831.3107 | 831.3115 | 4 | 10.9 | 0.96 | 88 ± 53 | [1-26] + 2 × (C16:0) / Double Palmitoylation |
| 665.2500 | 665.2499 | 5 | 10.9 | -0.15 | 12 ± 9.5 | [1-26] + 2 × (C16:0) / Double Palmitoylation |
| 1116.7503 | 1116.7505 | 3 | 11.0 | 0.18 | 55 ± 16 | [1-26] + 1 × (C16:0) + 1 × (C18:1)/ Palmitoylation + Oleoylation |
| 837.8146 | 837.8159 | 4 | 10.9 | 1.55 | 249 ± 114 | [1-26] + 1 × (C16:0) + 1 × (C18:1)/ Palmitoylation + Oleoylation |
| 670.4531 | 670.4542 | 5 | 10.9 | 1.64 | 44 ± 29 | [1-26] + 1 × (C16:0) + 1 × (C18:1)/ Palmitoylation + Oleoylation |
| 1125.4222 | 1125.4195 | 3 | 17.7 | -2.40 | 1 ± 0.1 | [1-26] + 2 × (C18:1) + / Labile Triple Oleoylation |
| 844.3185 | 844.3195 | 4 | 17.7 | 1.18 | 14 ± 0.1 | [1-26] + 2 × (C18:1) + / Labile Triple Oleoylation |
| 831.3107 | 831.3134 | 4 | 17.7 | 3.25 | 4 ± 2 | [1-26] + 2 × (C16:0) + / Labile Triple Palmitoylation |
| 1116.7503 | 1116.7491 | 3 | 17.7 | -1.07 | 2 ± 1 | [1-26] + 1 × (C16:0) + 1 × (C18:1)/ Labile (Palmitoylation + Oleoylation) |
| 837.8146 | 837.8154 | 4 | 17.7 | 0.95 | 15 ± 4 | [1-26] + 1 × (C16:0) + 1 × (C18:1)/ Labile (Palmitoylation + Oleoylation) |
| 670.4531 | 670.4537 | 5 | 17.8 | 0.89 | 1 ± 0.2 | [1-26] + 1 × (C16:0) + 1 × (C18:1)/ Labile (Palmitoylation + Oleoylation) |
| 1213.504 | 1213.5011 | 3 | 18.2 | -2.39 | 3 ± 1 | [1-26] + 3 × (C18:1) / Triple Oleoylation |
| 910.3798 | 910.3813 | 4 | 18.2 | 1.65 | 10 ± 3 | [1-26] + 3 × (C18:1) / Triple Oleoylation |
| 1187.4883 | 1187.4921 | 3 | 18.2 | 3.20 | 0.6 ± 0.4 | [1-26] + 3 × (C16:0) / Triple Palmitoylation |
| 890.8681 | 890.8680 | 4 | 18.1 | -0.11 | 3 ± 2 | [1-26] + 3 × (C16:0) / Triple Palmitoylation |
| 1204.8321 | 1204.8315 | 3 | 18.2 | -0.50 | 6 ± 4 | [1-26] + 2 × (C18:1) + 1 × (C16:0) / Double Oleoylation + Single Palmitoylation |
| 903.8759 | 903.8751 | 4 | 18.2 | -0.89 | 17 ± 13.5 | [1-26] + 2 × (C18:1) + 1 × (C16:0) / Double Oleoylation + Single Palmitoylation |
| 1196.1602 | 1196.1632 | 3 | 18.2 | 2.51 | 4 ± 3 | [1-26] + 2 × (C16:0) + 1 × (C18:1) / Double Palmitoylation + Single Oleoylation |
| 897.3720 | 897.3710 | 4 | 18.2 | -1.11 | 13 ± 10 | [1-26] + 2 × (C16:0) + 1 × (C18:1) / Double Palmitoylation + Single Oleoylation |

‡ Both theoretical and measured *m/z* values are monoisotopic. Theoretical mass obtained from mMass software (V5.5).

§ Errors reported as the SEM of peak area (*n*=3).

**Table S5. Ions produced by fragmenting double-palmitoylated melittin at *m/z* 832 (*z* = 4) at RT = 9.1 min of the EIC (see Fig. 3 and Fig. S5), LTQFT. Data are presented graphically in Fig. S6a.**

| b-Ions | *m/z* | *z* | Sequence Ladder† | y-Ions | *m/z* | *z* | Sequence Ladder† |
|---|---|---|---|---|---|---|---|
| b4 | 299.1 | 1 | H-GIGA.v | y19 | 1342.5 | 2 | k.VLTTGLPALI**S**WI**K**RKRQQ-$NH_2$ |
| b5 | 398.1 | 1 | H-GIGAV.l | y18 | 1293.2 | 2 | v.LTTGLPALI**S**WI**K**RKRQQ-$NH_2$ |
| b6 | 511.4 | 1 | H-GIGAVL.k | y17 | 1236.7 | 2 | l.TTGLPALI**S**WI**K**RKRQQ-$NH_2$ |
| b8 | 738.4 | 1 | H-GIGAVLKV.l | y16 | 1186.1 | 2 | t.TGLPALI**S**WI**K**RKRQQ-$NH_2$ |
| b9 | 851.5 | 1 | H-GIGAVLKVL.t | y15 | 1135.5 | 2 | t.GLPALI**S**WI**K**RKRQQ-$NH_2$ |
| b10 | 953.0 | 1 | H-GIGAVLKVLT.t | y14 | 1107.1 | 2 | g.LPALI**S**WI**K**RKRQQ-$NH_2$ |
| b12 | 1110.6 | 1 | H-GIGAVLKVLTTG.l | y13 | 1050.5 | 2 | l.PALI**S**WI**K**RKRQQ-$NH_2$ |
| b13 | 1223.7 | 1 | H-GIGAVLKVLTTGL.p | y12 | 1001.9 | 2 | p.ALI**S**WI**K**RKRQQ-$NH_2$ |
| b13 +$H_2O$ | 621.4 | 2 | H-GIGAVLKVLTTGL.p | y10 | 910.3 | 2 | l.I**S**WI**K**RKRQQ-$NH_2$ |
| | | | | y9 | 853.6 | 2 | i.**S**WI**K**RKRQQ-$NH_2$ |
| | | | | y7 | 598.1 | 2 | w.I**K**RKRQQ-$NH_2$ |
| | | | | y6 | 541.0 | 2 | i.**K**RKRQQ-$NH_2$ |
| | | | | y5 | 357.7 | 2 | k.RKRQQ-$NH_2$ |

† **Palmitoylation** sites within the amino acid sequence of the peptide are highlighted in **bold blue**.

**Table S6. Ions produced by fragmenting double-palmitoylated melittin at *m/z* 832 (*z* = 4) at RT = 9.4 min of the EIC (see Fig. 3 and Fig. S5), LTQFT. Data are presented graphically in Fig. S6b.**

| b-Ions | *m/z* | *z* | Sequence Ladder† | y-Ions | *m/z* | *z* | Sequence Ladder† |
|---|---|---|---|---|---|---|---|
| b4 | 299.3 | 1 | H-GIGA.v | y19 | 1342.9 | 2 | k.VLTTGLPALISWI**K**R**K**RQQ-$NH_2$ |
| b5 | 398.2 | 1 | H-GIGAV.l | y18 | 1293.1 | 2 | v.LTTGLPALISWI**K**R**K**RQQ-$NH_2$ |
| b6 | 511.3 | 1 | H-GIGAVL.k | y17 | 1236.7 | 2 | l.TTGLPALISWI**K**R**K**RQQ-$NH_2$ |
| b8 | 738.6 | 1 | H-GIGAVLKV.l | y16 | 1186.1 | 2 | t.TGLPALISWI**K**R**K**RQQ-$NH_2$ |
| b9 | 851.6 | 1 | H-GIGAVLKVL.t | y15 | 1135.5 | 2 | t.GLPALISWI**K**R**K**RQQ-$NH_2$ |
| b10 | 952.9 | 1 | H-GIGAVLKVLT.t | y14 | 1106.8 | 2 | g.LPALISWI**K**R**K**RQQ-$NH_2$ |
| b12 | 1110.7 | 1 | H-GIGAVLKVLTTG.l | y13 | 1050.2 | 2 | l.PALISWI**K**R**K**RQQ-$NH_2$ |
| b13 | 1223.6 | 1 | H-GIGAVLKVLTTGL.p | y12 | 1001.8 | 2 | p.ALISWI**K**R**K**RQQ-$NH_2$ |
| b13 +$H_2O$ | 621.5 | 2 | H-GIGAVLKVLTTGL.p | y11 | 966.2 | 2 | a.LISWI**K**R**K**RQQ-$NH_2$ |
| | | | | y10 | 910.0 | 2 | l.ISWI**K**R**K**RQQ-$NH_2$ |
| | | | | y9 | 853.6 | 2 | i.SWI**K**R**K**RQQ-$NH_2$ |
| | | | | y8 | 809.5 | 2 | s.WI**K**R**K**RQQ-$NH_2$ |
| | | | | y6 | 659.4 | 2 | i.**K**R**K**RQQ-$NH_2$ |

† **Palmitoylation** sites within the amino acid sequence of the peptide are highlighted in **bold blue**.

**Table S7. Ions produced by fragmenting double-palmitoylated melittin at *m/z* 832 (*z* = 4) at RT = 9.4 min of the EIC (see Fig. 3 and Fig. S5), LTQFT. Data are presented graphically in Fig. S6c.**

| b-Ions | *m/z* | *z* | Sequence Ladder† | y-Ions | *m/z* | *z* | Sequence Ladder† |
|---|---|---|---|---|---|---|---|
| b3 | 466.2 | 1 | H-**G**IG.a | y19 | 1223.6 | 2 | k.VLTTGLPALISWI**K**RKRQQ-$NH_2$ |
| b4 | 537.3 | 1 | H-**G**IGA.v | y18 | 1174.0 | 2 | v.LTTGLPALISWI**K**RKRQQ-$NH_2$ |
| b5 | 636.2 | 1 | H-**G**IGAV.l | y17 | 1117.5 | 2 | l.TTGLPALISWI**K**RKRQQ-$NH_2$ |
| b6 | 749.2 | 1 | H-**G**IGAVL.k | y16 | 1066.9 | 2 | t.TGLPALISWI**K**RKRQQ-$NH_2$ |
| b7 | 877.4 | 1 | H-**G**IGAVLK.v | y15 | 1016.1 | 2 | t.GLPALISWI**K**RKRQQ-$NH_2$ |
| b8 | 976.1 | 1 | H-**G**IGAVLKV.l | y14 | 987.8 | 2 | g.LPALISWI**K**RKRQQ-$NH_2$ |
| b9 | 1089.6 | 1 | H-**G**IGAVLKVL.t | y13 | 931.1 | 2 | l.PALISWI**K**RKRQQ-$NH_2$ |
| b10 | 1190.9 | 1 | H-**G**IGAVLKVLT.t | y12 | 883.0 | 2 | p.ALISWI**K**RKRQQ-$NH_2$ |
| b12 | 1348.6 | 1 | H-**G**IGAVLKVLTTG.l | y11 | 847.3 | 2 | a.LISWI**K**RKRQQ-$NH_2$ |
| b12 - $H_2O$ | 1330.7 | 1 | H-**G**IGAVLKVLTTG.l | y10 | 790.6 | 2 | l.ISWI**K**RKRQQ-$NH_2$ |
| b12 - $H_2O$ | 666.0 | 2 | H-**G**IGAVLKVLTTG.l | y9 | 734.1 | 2 | i.SWI**K**RKRQQ-$NH_2$ |
| b13 | 1461.5 | 1 | H-**G**IGAVLKVLTTGL.p | y6 | 1080.1 | 1 | i.**K**RKRQQ-$NH_2$ |
| b13 - $H_2O$ | 1443.7 | 1 | H-**G**IGAVLKVLTTGL.p | y4 | 558.3 | 1 | r.KRQQ-$NH_2$ |
| b15 | 816.1 | 2 | H-**G**IGAVLKVLTTGLPA.l | y4 – $NH_3$ | 541.8 | 1 | r.KRQQ-$NH_2$ |
| b18 | 972.6 | 2 | H-**G**IGAVLKVLTTGLPALIS.w | | | | |

† **Palmitoylation** sites within the amino acid sequence of the peptide are highlighted in **bold blue**.

**Table S8. Ions produced by fragmenting double-palmitoylated melittin at *m/z* 832 (*z* = 4) at RT = 10.1 min of the EIC (see Fig. 3 and Fig. S5), LTQFT. Data are presented graphically in Fig. S7b.**

| b-Ions | *m/z* | *z* | Sequence Ladder† | y-Ions | *m/z* | *z* | Sequence Ladder† |
|---|---|---|---|---|---|---|---|
| b4 | 299.1 | 1 | H-GIGA.v | y19 | 1223.7 | 2 | k.VLTTGLPALISWI**K**RKRQQ-$NH_2$ |
| b5 | 398.2 | 1 | H-GIGAV.l | y18 | 1173.9 | 2 | v.LTTGLPALISWI**K**RKRQQ-$NH_2$ |
| b6 | 511.3 | 1 | H-GIGAVL.k | y17 | 1117.4 | 2 | l.TTGLPALISWI**K**RKRQQ-$NH_2$ |
| b7 | 877.6 | 1 | H-GIGAVL**K**.v | y16 | 1066.8 | 2 | t.TGLPALISWI**K**RKRQQ-$NH_2$ |
| b8 | 976.5 | 1 | H-GIGAVL**K**V.l | y15 | 1016.5 | 2 | t.GLPALISWI**K**RKRQQ-$NH_2$ |
| b9 | 1089.7 | 1 | H-GIGAVL**K**VL.t | y14 | 987.9 | 2 | g.LPALISWI**K**RKRQQ-$NH_2$ |
| b10 | 1190.6 | 1 | H-GIGAVL**K**VLT.t | y13 | 931.2 | 2 | l.PALISWI**K**RKRQQ-$NH_2$ |
| b11 | 1291.6 | 1 | H-GIGAVL**K**VLTT.g | y12 | 882.7 | 2 | p.ALISWI**K**RKRQQ-$NH_2$ |
| b12 | 1348.7 | 1 | H-GIGAVL**K**VLTTG.l | y11 | 847.2 | 2 | a.LISWI**K**RKRQQ-$NH_2$ |
| b12 – $H_2O$ | 1330.7 | 1 | H-GIGAVL**K**VLTT G.l | y10 | 790.8 | 2 | l.ISWI**K**RKRQQ-$NH_2$ |
| b12 – $H_2O$ | 666.0 | 2 | H-GIGAVL**K**VLTT G.l | y9 | 734.0 | 2 | i.SWI**K**RKRQQ-$NH_2$ |
| b13 | 1461.8 | 1 | H-GIGAVL**K**VLTTGL.p | y8 | 734.0 | 2 | s.WI**K**RKRQQ-NH2 |
| b13 – $H_2O$ | 1443.7 | 1 | H-GIGAVL**K**VLTTGL.p | y7 | 597.2 | 2 | w.I**K**RKRQQ-$NH_2$ |
| b15 | 816.2 | 2 | H-GIGAVL**K**VLTTGLPA.l | y6 | 541.1 | 2 | i.**K**RKRQQ-$NH_2$ |
| b18 | 972.2 | 2 | H-GIGAVL**K**VLTTGLPALIS.w | y4 - $NH_3$ | 271.2 | 2 | r.KRQQ-$NH_2$ |

† **Palmitoylation** sites within the amino acid sequence of the peptide are highlighted in **bold blue**.

**Table S9. Ions produced by fragmenting double-palmitoylated melittin at *m/z* 832 (*z* = 4) at RT = 10.6 min of the EIC (see Fig. 3 and Fig. S5), LTQFT. Data are presented graphically in Fig. S7a.**

| b-Ions | *m/z* | *z* | Sequence Ladder† | y-Ions | *m/z* | *z* | Sequence Ladder† |
|---|---|---|---|---|---|---|---|
| b3 | 466.2 | 1 | H-**G**IG.a | y19 | 1223.6 | 2 | k.VLTTGLPALISWIKR**K**RQQ-$NH_2$ |
| b4 | 537.2 | 1 | H-**G**IGA.v | y18 | 1173.9 | 2 | v.LTTGLPALISWIKR**K**RQQ-$NH_2$ |
| b5 | 636.2 | 1 | H-**G**IGAV.l | y17 | 1117.5 | 2 | l.TTGLPALISWIKR**K**RQQ-$NH_2$ |
| b6 | 749.3 | 1 | H-**G**IGAVL.k | y16 | 1067.0 | 2 | t.TGLPALISWIKR**K**RQQ-$NH_2$ |
| b7 | 877.3 | 1 | H-**G**IGAVLK.v | y15 | 1016.5 | 2 | t.GLPALISWIKR**K**RQQ-$NH_2$ |
| b8 | 976.7 | 1 | H-**G**IGAVLKV.l | y14 | 987.9 | 2 | g.LPALISWIKR**K**RQQ-$NH_2$ |
| b9 | 1089.6 | 1 | H-**G**IGAVLKVL.t | y13 | 931.4 | 2 | l.PALISWIKR**K**RQQ-$NH_2$ |
| b10 | 1190.6 | 1 | H-**G**IGAVLKVLT.t | y12 | 882.7 | 2 | p.ALISWIKR**K**RQQ-$NH_2$ |
| b12 | 1348.6 | 1 | H-**G**IGAVLKVLTTG.l | y11 | 847.4 | 2 | a.LISWIKR**K**RQQ-$NH_2$ |
| b12 - $H_2O$ | 1330.6 | 1 | H-**G**IGAVLKVLTTG.l | y10 | 790.6 | 2 | l.ISWIKR**K**RQQ-$NH_2$ |
| b12 - $H_2O$ | 666.0 | 2 | H-**G**IGAVLKVLTTG.l | y9 | 734.2 | 2 | i.SWIKR**K**RQQ-$NH_2$ |
| b13 | 1461.4 | 1 | H-**G**IGAVLKVLTTGL.p | y5 | 477.3 | 2 | k.R**K**RQQ-$NH_2$ |
| b13 - $H_2O$ | 1443.7 | 1 | H-**G**IGAVLKVLTTGL.p | y4 | 398.2 | 2 | r.**K**RQQ-$NH_2$ |
| b15 | 816.1 | 2 | H-**G**IGAVLKVLTTGLPA.l | | | | |
| b18 | 972.7 | 2 | H-**G**IGAVLKVLTTGLPALIS.w | | | | |

† **Palmitoylation** sites within the amino acid sequence of the peptide are highlighted in **bold blue**.

**Table S10. Ions produced by fragmenting double-palmitoylated melittin at *m/z* 832 (*z* = 4) at RT = 10.9 min of the EIC (see Fig. 3 and Fig. S5), LTQFT. Data are presented graphically in Fig. S8a.**

| b-Ions | *m/z* | *z* | Sequence Ladder† | y-Ions | *m/z* | *z* | Sequence Ladder† |
|---|---|---|---|---|---|---|---|
| b3 | 466.2 | 1 | H-**G**IG.a | y19 | 1223.7 | 2 | k.VLTTGLPALISWIK**R**KRQQ-$NH_2$ |
| b4 | 537.2 | 1 | H-**G**IGA.v | y18 | 1173.8 | 2 | v.LTTGLPALISWIK**R**KRQQ-$NH_2$ |
| b5 | 636.3 | 1 | H-**G**IGAV.l | y17 | 1117.5 | 2 | l.TTGLPALISWIK**R**KRQQ-$NH_2$ |
| b6 | 749.4 | 1 | H-**G**IGAVL.k | y16 | 1067.1 | 2 | t.TGLPALISWIK**R**KRQQ-$NH_2$ |
| b7 | 877.5 | 1 | H-**G**IGAVLK.v | y15 | 1016.5 | 2 | t.GLPALISWIK**R**KRQQ-$NH_2$ |
| b7 | 439.7 | 2 | H-**G**IGAVLK.v | y14 | 987.9 | 2 | g.LPALISWIK**R**KRQQ-$NH_2$ |
| b8 | 976.6 | 1 | H-**G**IGAVLKV.l | y13 | 931.5 | 2 | l.PALISWIK**R**KRQQ-$NH_2$ |
| b9 | 1089.6 | 1 | H-**G**IGAVLKVL.t | y12 | 882.9 | 2 | p.ALISWIK**R**KRQQ-$NH_2$ |
| b10 | 1190.4 | 1 | H-**G**IGAVLKVLT.t | y11 | 847.4 | 2 | a.LISWIK**R**KRQQ-$NH_2$ |
| b12 | 1348.7 | 1 | H-**G**IGAVLKVLTTG.l | y10 | 790.8 | 2 | l.ISWIK**R**KRQQ-$NH_2$ |
| b12 - $H_2O$ | 1330.7 | 1 | H-**G**IGAVLKVLTTG.l | y9 | 734.0 | 2 | i.SWIK**R**KRQQ-$NH_2$ |
| b12 - $H_2O$ | 665.9 | 2 | H-**G**IGAVLKVLTTG.l | y5 | 477.1 | 2 | k.**R**KRQQ-$NH_2$ |
| b13 | 1461.8 | 1 | H-**G**IGAVLKVLTTGL.p | | | | |
| b13 - $H_2O$ | 1443.8 | 1 | H-**G**IGAVLKVLTTGL.p | | | | |
| b15 | 815.9 | 2 | H-**G**IGAVLKVLTTGLPA.l | | | | |
| b18 | 972.4 | 2 | H-**G**IGAVLKVLTTGLPALIS.w | | | | |

† **Palmitoylation** sites within the amino acid sequence of the peptide are highlighted in **bold blue**.

**Table S11. Ions produced by fragmenting double-palmitoylated melittin at *m/z* 832 (*z* = 4) at RT = 11.2 min of the EIC (see Fig. 3 and Fig. S5), LTQFT. Data are presented graphically in Fig. S8b.**

| b-Ions | *m/z* | *z* | Sequence Ladder† | y-Ions | *m/z* | *z* | Sequence Ladder† |
|---|---|---|---|---|---|---|---|
| b3 | 466.2 | 1 | H-**G**IG.a | y19 | 1223.4 | 2 | k.VLTTGLPALISWIKRK**R**QQ-$NH_2$ |
| b4 | 537.1 | 1 | H-**G**IGA.v | y18 | 1173.8 | 2 | v.LTTGLPALISWIKRK**R**QQ-$NH_2$ |
| b5 | 636.3 | 1 | H-**G**IGAV.l | y17 | 1117.4 | 2 | l.TTGLPALISWIKRK**R**QQ-$NH_2$ |
| b6 | 749.4 | 1 | H-**G**IGAVL.k | y16 | 1067.4 | 2 | t.TGLPALISWIKRK**R**QQ-$NH_2$ |
| b7 | 877.6 | 1 | H-**G**IGAVLK.v | y15 | 1016.5 | 2 | t.GLPALISWIKRK**R**QQ-$NH_2$ |
| b7 | 439.4 | 2 | H-**G**IGAVLK.v | y14 | 987.9 | 2 | g.LPALISWIKRK**R**QQ-$NH_2$ |
| b8 | 976.6 | 1 | H-**G**IGAVLKV.l | y13 | 931.5 | 2 | l.PALISWIKRK**R**QQ-$NH_2$ |
| b9 | 1089.7 | 1 | H-**G**IGAVLKVL.t | y12 | 882.7 | 2 | p.ALISWIKRK**R**QQ-$NH_2$ |
| b10 | 1190.7 | 1 | H-**G**IGAVLKVLT.t | y11 | 847.5 | 2 | a.LISWIKRK**R**QQ-$NH_2$ |
| b12 | 1348.7 | 1 | H-**G**IGAVLKVLTTG.l | y10 | 790.3 | 2 | l.ISWIKRK**R**QQ-$NH_2$ |
| b12 - $H_2O$ | 1330.8 | 1 | H-**G**IGAVLKVLTTG.l | y9 | 733.3 | 2 | i.SWIKRK**R**QQ-$NH_2$ |
| b12 - $H_2O$ | 665.9 | 2 | H-**G**IGAVLKVLTTG.l | y8 - $NH_3$ | 681.4 | 2 | s.WIK**R**QQ-$NH_2$ |
| b13 | 1461.8 | 1 | H-**G**IGAVLKVLTTGL.p | y5 | 477.1 | 2 | k.RK**R**QQ-$NH_2$ |
| b13 - $H_2O$ | 1443.8 | 1 | H-**G**IGAVLKVLTTGL.p | y5 - $NH_3$ | 468.5 | 2 | k.RK**R**QQ-$NH_2$ |
| b15 | 816.3 | 2 | H-**G**IGAVLKVLTTGLPA.l | y4 - $NH_3$ | 390.5 | 2 | r.K**R**QQ-$NH_2$ |
| b18 | 972.3 | 2 | H-**G**IGAVLKVLTTGLPALIS.w | | | | |

† **Palmitoylation** sites within the amino acid sequence of the peptide are highlighted in **bold blue**.

**Table S12. Ions produced by fragmenting double-oleoylated melittin at *m/z* 845 (*z* = 4) at RT = 9.2 min of the EIC (see Fig. 2, Fig. 3 and Fig. S9), LTQFT. Data are presented graphically in Fig. S10a.**

| b-Ions | *m/z* | *z* | Sequence Ladder‡ | y-Ions | *m/z* | *z* | Sequence Ladder‡ |
|---|---|---|---|---|---|---|---|
| b4 | 299.1 | 1 | H-GIGA.v | y19 | 1368.6 | 2 | k.VLTTGLPALI**S**WI**K**RKRQQ-$NH_2$ |
| b5 | 398.2 | 1 | H-GIGAV.l | y18 | 1318.6 | 2 | v.LTTGLPALI**S**WI**K**RKRQQ-$NH_2$ |
| b6 | 511.3 | 1 | H-GIGAVL.k | y17 | 1262.6 | 2 | l.TTGLPALI**S**WI**K**RKRQQ-$NH_2$ |
| b12 | 1348.7 | 1 | H-GIGAVLKVLTTG.l | y16 | 1211.8 | 2 | t.TGLPALI**S**WI**K**RKRQQ-$NH_2$ |
| b13 | 1461.8 | 1 | H-GIGAVLKVLTTGL.p | y15 | 1161.6 | 2 | t.GLPALI**S**WI**K**RKRQQ-$NH_2$ |
| | | | | y14 | 1132.0 | 2 | g.LPALI**S**WI**K**RKRQQ-$NH_2$ |
| | | | | y13 | 1076.1 | 2 | l.PALI**S**WI**K**RKRQQ-$NH_2$ |
| | | | | y13 - $H_2O$ | 1066.9 | 2 | l.PALI**S**WI**K**RKRQQ-$NH_2$ |
| | | | | y12 | 1027.4 | 2 | p.ALI**S**WI**K**RKRQQ-$NH_2$ |
| | | | | y11 | 992.4 | 2 | a.LI**S**WI**K**RKRQQ-$NH_2$ |
| | | | | y10 | 935.6 | 2 | l.I**S**WI**K**RKRQQ-$NH_2$ |
| | | | | y7 | 610.3 | 2 | w.I**K**RKRQQ-$NH_2$ |
| | | | | y6 | 554.2 | 2 | i.**K**RKRQQ-$NH_2$ |
| | | | | y5 | 714.4 | 1 | k.RKRQQ-$NH_2$ |

‡ **Oleoylation** sites within the amino acid sequence of the peptide are highlighted in **bold red**.

**Table S13. Ions produced by fragmenting double-oleoylated melittin at *m/z* 845 (*z* = 4) at RT = 9.6 min of the EIC (see Fig. 2, Fig. 3 and Fig. S9), LTQFT. Data are presented graphically in Fig. S10b.**

| b-Ions | *m/z* | *z* | Sequence Ladder‡ | y-Ions | *m/z* | *z* | Sequence Ladder‡ |
|---|---|---|---|---|---|---|---|
| b4 | 299.1 | 1 | H-GIGA.v | y19 | 1368.7 | 2 | k.VLTTGLPALISWI**K**R**K**RQQ-$NH_2$ |
| b5 | 398.2 | 1 | H-GIGAV.l | y18 | 1318.9 | 2 | v.LTTGLPALISWI**K**R**K**RQQ-NH2 |
| b6 | 511.3 | 1 | H-GIGAVL.k | y17 | 1262.7 | 2 | l.TTGLPALISWI**K**R**K**RQQ-$NH_2$ |
| b10 | 952.5 | 1 | H-GIGAVLKVLT.t | y16 | 1211.9 | 2 | t.TGLPALISWI**K**R**K**RQQ-$NH_2$ |
| b12 | 1110.6 | 1 | H-GIGAVLKVLTTG.l | y15 | 1161.5 | 2 | t.GLPALISWI**K**R**K**RQQ-$NH_2$ |
| b13 | 1223.6 | 1 | H-GIGAVLKVLTTGL.p | y14 | 1132.8 | 2 | g.LPALISWI**K**R**K**RQQ-$NH_2$ |
| | | | | y13 | 1076.6 | 2 | l.PALISWI**K**R**K**RQQ-$NH_2$ |
| | | | | y13-$H_2O$ | 1067.6 | 2 | l.PALISWI**K**R**K**RQQ-$NH_2$ |
| | | | | y12 | 1027.5 | 2 | p.ALISWI**K**R**K**RQQ-$NH_2$ |
| | | | | y11 | 992.8 | 2 | a.LISWI**K**R**K**RQQ-$NH_2$ |
| | | | | y10 | 935.9 | 2 | l.ISWI**K**R**K**RQQ-$NH_2$ |
| | | | | y8 | 835.8 | 2 | s.WI**K**R**K**RQQ-$NH_2$ |
| | | | | y7 | 742.2 | 2 | w.I**K**R**K**RQQ-$NH_2$ |
| | | | | y5 | 490.3 | 2 | k.R**K**RQQ-$NH_2$ |

‡ **Oleoylation** sites within the amino acid sequence of the peptide are highlighted in **bold red**.

**Table S14. Ions produced by fragmenting double-oleoylated melittin at *m/z* 845 (*z* = 4) at RT = 9.6 min of the EIC (see Fig. 2, Fig. 3 and Fig. S9), LTQFT. Data are presented graphically in Fig. S10c.**

| b-Ions | *m/z* | *z* | Sequence Ladder‡ | y-Ions | *m/z* | *z* | Sequence Ladder‡ |
|---|---|---|---|---|---|---|---|
| b3 | 492.3 | 1 | H-**G**IG.a | y21 | 1356.6 | 2 | v.LKVLTTGLPALISWI**K**RKRQQ-$NH_2$ |
| b4 | 563.2 | 1 | H-**G**IGA.v | y19 | 1236.4 | 2 | k.VLTTGLPALISWI**K**RKRQQ-$NH_2$ |
| b5 | 662.3 | 1 | H-**G**IGAV.l | y18 | 1187.0 | 2 | v.LTTGLPALISWI**K**RKRQQ-$NH_2$ |
| b6 | 775.3 | 1 | H-**G**IGAVL.k | y17 | 1130.5 | 2 | l.TTGLPALISWI**K**RKRQQ-$NH_2$ |
| b7 | 903.4 | 1 | H-**G**IGAVLK.v | y16 | 1079.8 | 2 | t.TGLPALISWI**K**RKRQQ-$NH_2$ |
| b8 | 1002.6 | 1 | H-**G**IGAVLKV.l | y15 | 1029.4 | 2 | t.GLPALISWI**K**RKRQQ-$NH_2$ |
| b9 | 1115.6 | 1 | H-**G**IGAVLKVL.t | y14 | 1001.0 | 2 | g.LPALISWI**K**RKRQQ-$NH_2$ |
| b10 | 1216.7 | 1 | H-**G**IGAVLKVLT.t | y13 | 944.4 | 2 | l.PALISWI**K**RKRQQ-$NH_2$ |
| b12 | 1374.7 | 1 | H-**G**IGAVLKVLTTG.l | y12 | 895.2 | 2 | p.ALISWI**K**RKRQQ-$NH_2$ |
| b13 | 1487.8 | 1 | H-**G**IGAVLKVLTTGL.p | y11 | 860.4 | 2 | a.LISWI**K**RKRQQ-$NH_2$ |
| | | | | y10 | 803.3 | 2 | l.ISWI**K**RKRQQ-$NH_2$ |
| | | | | y9 | 746.9 | 2 | i.SWI**K**RKRQQ-$NH_2$ |
| | | | | y8 | 703.7 | 2 | s.WI**K**RKRQQ-$NH_2$ |
| | | | | y7 | 609.2 | 2 | w.I**K**RKRQQ-$NH_2$ |
| | | | | y5 | 714.5 | 1 | k.RKRQQ-$NH_2$ |
| | | | | y4 | 558.5 | 1 | r.KRQQ-$NH_2$ |

‡ **Oleoylation** sites within the amino acid sequence of the peptide are highlighted in **bold red**.

**Table S15. Ions produced by fragmenting double-oleoylated melittin at *m/z* 845 (*z* = 4) at RT = 10.2 min of the EIC (see Fig. 2, Fig. 3 and Fig. S9), LTQFT. Data are presented graphically in Fig. S11a.**

| b-Ions | *m/z* | *z* | Sequence Ladder‡ | y-Ions | *m/z* | *z* | Sequence Ladder‡ |
|---|---|---|---|---|---|---|---|
| b4 | 299.1 | 1 | H-GIGA.v | y20 | 1432.5 | 2 | l.KVLTTGLPALISWI**K**RKRQQ-$NH_2$ |
| b5 | 398.2 | 1 | H-GIGAV.l | y19 | 1236.7 | 2 | k.VLTTGLPALISWI**K**RKRQQ-$NH_2$ |
| b6 | 511.3 | 1 | H-GIGAVL.k | y18 | 1187.0 | 2 | v.LTTGLPALISWI**K**RKRQQ-$NH_2$ |
| b7 | 903.5 | 1 | H-GIGAVL**K**.v | y17 | 1130.5 | 2 | l.TTGLPALISWI**K**RKRQQ-$NH_2$ |
| b8 | 1002.6 | 1 | H-GIGAVL**K**V.l | y16 | 1079.6 | 2 | t.TGLPALISWI**K**RKRQQ-$NH_2$ |
| b9 | 1115.7 | 1 | H-GIGAVL**K**VL.t | y16 – $H_2O$ | 1069.1 | 2 | t.TGLPALISWI**K**RKRQQ-$NH_2$ |
| b10 | 1216.6 | 1 | H-GIGAVL**K**VLT.t | y15 | 1029.2 | 2 | t.GLPALISWI**K**RKRQQ-$NH_2$ |
| b11 | 1317.8 | 1 | H-GIGAVL**K**VLTT.g | y14 | 1000.7 | 2 | g.LPALISWI**K**RKRQQ-$NH_2$ |
| b12 | 1374.7 | 1 | H-GIGAVL**K**VLTTG.l | y13 | 944.4 | 2 | l.PALISWI**K**RKRQQ-$NH_2$ |
| b13 | 1487.8 | 1 | H-GIGAVL**K**VLTTGL.p | y12 | 895.8 | 2 | p.ALISWI**K**RKRQQ-$NH_2$ |
| b13 + $H_2O$ | 754.3 | 2 | H-GIGAVL**K**VLTTGL.p | y11 | 860.4 | 2 | a.LISWI**K**RKRQQ-$NH_2$ |
| b18+ $H_2O$ | 993.9 | 2 | H-GIGAVL**K**VLTTGLPALIS.w | y10 | 804.2 | 2 | l.ISWI**K**RKRQQ-$NH_2$ |
| | | | | y9 | 747.6 | 2 | i.SWI**K**RKRQQ-$NH_2$ |
| | | | | y8 | 703.8 | 2 | s.WI**K**RKRQQ-$NH_2$ |
| | | | | y7 | 609.2 | 2 | w.I**K**RKRQQ-$NH_2$ |
| | | | | y6 | 553.5 | 2 | i.**K**RKRQQ-$NH_2$ |
| | | | | y4 - $NH_3$ | 271.2 | 2 | r.KRQQ-$NH_2$ |

‡ **Oleoylation** sites within the amino acid sequence of the peptide are highlighted in **bold red**.

**Table S16. Ions produced by fragmenting double-oleoylated melittin at *m/z* 845 (*z* = 4) at RT = 10.6 min of the EIC (see Fig. 2, Fig. 3 and Fig. S9), LTQFT. Data are presented graphically in Fig. S11b.**

| b-Ions | *m/z* | *z* | Sequence Ladder‡ | y-Ions | *m/z* | *z* | Sequence Ladder‡ |
|---|---|---|---|---|---|---|---|
| b3 | 492.3 | 1 | H-**G**IG.a | y21 | 1356.7 | 2 | v.LKVLTTGLPALISWIKR**K**RQQ-$NH_2$ |
| b4 | 563.3 | 1 | H-**G**IGA.v | y19 | 1236.4 | 2 | k.VLTTGLPALISWIKR**K**RQQ-$NH_2$ |
| b5 | 662.3 | 1 | H-**G**IGAV.l | y18 | 1187.0 | 2 | v.LTTGLPALISWIKR**K**RQQ-$NH_2$ |
| b6 | 775.3 | 1 | H-**G**IGAVL.k | y17 | 1130.2 | 2 | l.TTGLPALISWIKR**K**RQQ-$NH_2$ |
| b7 | 903.6 | 1 | H-**G**IGAVLK.v | y16 | 1079.7 | 2 | t.TGLPALISWIKR**K**RQQ-$NH_2$ |
| b8 | 1002.5 | 1 | H-**G**IGAVLKV.l | y15 | 1029.4 | 2 | t.GLPALISWIKR**K**RQQ-$NH_2$ |
| b9 | 1115.6 | 1 | H-**G**IGAVLKVL.t | y14 | 1000.9 | 2 | g.LPALISWIKR**K**RQQ-$NH_2$ |
| b10 | 1216.7 | 1 | H-**G**IGAVLKVLT.t | y13 | 944.5 | 2 | l.PALISWIKR**K**RQQ-$NH_2$ |
| b12 | 1374.7 | 1 | H-**G**IGAVLKVLTTG.l | y12 | 895.8 | 2 | p.ALISWIKR**K**RQQ-$NH_2$ |
| b13 | 1488.0 | 1 | H-**G**IGAVLKVLTTGL.p | y11 | 860.4 | 2 | a.LISWIKR**K**RQQ-$NH_2$ |
| | | | | y10 | 803.7 | 2 | l.ISWIKR**K**RQQ-$NH_2$ |
| | | | | y9 | 747.1 | 2 | i.SWIKR**K**RQQ-$NH_2$ |
| | | | | y8 | 703.8 | 2 | s.WIKR**K**RQQ-$NH_2$ |
| | | | | y7 | 609.1 | 2 | w.IKR**K**RQQ-$NH_2$ |
| | | | | y5 | 490.0 | 2 | k.R**K**RQQ-$NH_2$ |
| | | | | y4 | 822.9 | 1 | r.**K**RQQ-$NH_2$ |
| | | | | y4 - $NH_3$ | 806.1 | 1 | r.**K**RQQ-$NH_2$ |

‡ **Oleoylation** sites within the amino acid sequence of the peptide are highlighted in **bold red**.

**Table S17. Ions produced by fragmenting double-oleoylated melittin at *m/z* 845 (*z* = 4) at RT = 10.9 min of the EIC (see Fig. 2, Fig. 3 and Fig. S9), LTQFT. Data are presented graphically in Fig. S12a.**

| b-Ions | *m/z* | *z* | Sequence Ladder‡ | y-Ions | *m/z* | *z* | Sequence Ladder‡ |
|---|---|---|---|---|---|---|---|
| b3 | 492.3 | 1 | H-**G**IG.a | y21 | 1356.7 | 2 | v.LKVLTTGLPALISWIK**R**KRQQ-$NH_2$ |
| b4 | 563.2 | 1 | H-**G**IGA.v | y19 | 1236.5 | 2 | k.VLTTGLPALISWIK**R**KRQQ-$NH_2$ |
| b5 | 662.3 | 1 | H-**G**IGAV.l | y18 | 1187.5 | 2 | v.LTTGLPALISWIK**R**KRQQ-$NH_2$ |
| b6 | 775.2 | 1 | H-**G**IGAVL.k | y17 | 1130.6 | 2 | l.TTGLPALISWIK**R**KRQQ-$NH_2$ |
| b7 | 903.4 | 1 | H-**G**IGAVLK.v | y16 | 1080.2 | 2 | t.TGLPALISWIK**R**KRQQ-$NH_2$ |
| b8 | 1002.7 | 1 | H-**G**IGAVLKV.l | y15 | 1029.6 | 2 | t.GLPALISWIK**R**KRQQ-$NH_2$ |
| b9 | 1115.6 | 1 | H-**G**IGAVLKVL.t | y14 | 1001.0 | 2 | g.LPALISWIK**R**KRQQ-$NH_2$ |
| b10 | 1216.7 | 1 | H-**G**IGAVLKVLT.t | y13 | 944.4 | 2 | l.PALISWIK**R**KRQQ-$NH_2$ |
| b12 | 1374.7 | 1 | H-**G**IGAVLKVLTTG.l | y12 | 895.6 | 2 | p.ALISWIK**R**KRQQ-$NH_2$ |
| b13 | 1487.9 | 1 | H-**G**IGAVLKVLTTGL.p | y11 | 860.0 | 2 | a.LISWIK**R**KRQQ-$NH_2$ |
| | | | | y10 | 803.8 | 2 | l.ISWIK**R**KRQQ-$NH_2$ |
| | | | | y9 | 747.5 | 2 | i.SWIK**R**KRQQ-$NH_2$ |
| | | | | y8 | 703.7 | 2 | s.WIK**R**KRQQ-$NH_2$ |
| | | | | y7 | 609.1 | 2 | w.IK**R**KRQQ-$NH_2$ |
| | | | | y5 | 490.1 | 2 | k.R**K**RQQ-$NH_2$ |
| | | | | y4 | 558.5 | 1 | r.KRQQ-$NH_2$ |

‡ **Oleoylation** sites within the amino acid sequence of the peptide are highlighted in **bold red**.

**Table S18. Ions produced by fragmenting double-oleoylated melittin at *m/z* 845 (*z* = 4) at RT = 11.2 min of the EIC (see Fig. 2, Fig. 3 and Fig. S9), LTQFT. Data are presented graphically in Fig. S12b.**

| b-Ions | *m/z* | *z* | Sequence Ladder‡ | y-Ions | *m/z* | *z* | Sequence Ladder‡ |
|---|---|---|---|---|---|---|---|
| b3 | 492.3 | 1 | H-**G**IG.a | y21 | 1356.9 | 2 | v.LKVLTTGLPALISWIKRK**R**QQ-$NH_2$ |
| b4 | 563.1 | 1 | H-**G**IGA.v | y19 | 1236.1 | 2 | k.VLTTGLPALISWIKRK**R**QQ-$NH_2$ |
| b5 | 662.3 | 1 | H-**G**IGAV.l | y18 | 1187.0 | 2 | v.LTTGLPALISWIKRK**R**QQ-$NH_2$ |
| b6 | 775.4 | 1 | H-**G**IGAVL.k | y17 | 1130.4 | 2 | l.TTGLPALISWIKRK**R**QQ-$NH_2$ |
| b7 | 903.5 | 1 | H-**G**IGAVLK.v | y16 | 1079.7 | 2 | t.TGLPALISWIKRK**R**QQ-$NH_2$ |
| b8 | 1002.6 | 1 | H-**G**IGAVLKV.l | y15 | 1029.1 | 2 | t.GLPALISWIKRK**R**QQ-$NH_2$ |
| b9 | 1115.7 | 1 | H-**G**IGAVLKVL.t | y14 | 1001.1 | 2 | g.LPALISWIKRK**R**QQ-$NH_2$ |
| b10 | 1216.8 | 1 | H-**G**IGAVLKVLT.t | y13 | 944.4 | 2 | l.PALISWIKRK**R**QQ-$NH_2$ |
| b12 | 1374.7 | 1 | H-**G**IGAVLKVLTTG.l | y12 | 895.7 | 2 | p.ALISWIKRK**R**QQ-$NH_2$ |
| b13 | 1487.9 | 1 | H-**G**IGAVLKVLTTGL.p | y11 | 860.5 | 2 | a.LISWIKRK**R**QQ-$NH_2$ |
| | | | | y10 | 803.8 | 2 | l.ISWIKRK**R**QQ-$NH_2$ |
| | | | | y9 | 747.3 | 2 | i.SWIKRK**R**QQ-$NH_2$ |
| | | | | y8 | 703.7 | 2 | s.WIKRK**R**QQ-$NH_2$ |
| | | | | y7 | 609.1 | 2 | w.IKRK**R**QQ-$NH_2$ |
| | | | | y5 | 490.4 | 2 | k.RK**R**QQ-$NH_2$ |
| | | | | y4 | 822.8 | 1 | r.K**R**QQ-$NH_2$ |

‡ **Oleoylation** sites within the amino acid sequence of the peptide are highlighted in **bold red**.

**Table S19. Ions produced by fragmenting melittin modified by 1 oleoyl group + 1 palmitoyl group at *m/z* 838 (*z* = 4) at RT = 9.1 min of the EIC (see Fig. 3 and Fig. S13), LTQFT. Data are presented graphically in Fig. S14a.**

| b-Ions | *m/z* | *z* | Sequence Ladder¶ | y-Ions | *m/z* | *z* | Sequence Ladder¶ |
|---|---|---|---|---|---|---|---|
| b4 | 299.2 | 1 | H-GIGA.v | y20 | 1419.9 | 2 | l.KVLTTGLPALI**S**WI**K**RKRQQ-$NH_2$ |
| b5 | 398.2 | 1 | H-GIGAV.l | y19 | 1355.7 | 2 | k.VLTTGLPALI**S**WI**K**RKRQQ-$NH_2$ |
| b6 | 511.3 | 1 | H-GIGAVL.k | y18 | 1306.5 | 2 | v.LTTGLPALI**S**WI**K**RKRQQ-$NH_2$ |
| b8 | 738.8 | 1 | H-GIGAVLKV.l | y17 | 1249.5 | 2 | l.TTGLPALI**S**WI**K**RKRQQ-$NH_2$ |
| b9 | 851.6 | 1 | H-GIGAVLKVL.t | y16 | 1199.0 | 2 | t.TGLPALI**S**WI**K**RKRQQ-$NH_2$ |
| b12 | 1110.8 | 1 | H-GIGAVLKVLTTG.l | y15 | 1148.7 | 2 | t.GLPALI**S**WI**K**RKRQQ-$NH_2$ |
| b13 | 1223.7 | 1 | H-GIGAVLKVLTTGL.p | y14 | 1119.2 | 2 | g.LPALI**S**WI**K**RKRQQ-$NH_2$ |
| b13 + $H_2O$ | 621.4 | 2 | H-GIGAVLKVLTTGL.p | y13 | 1063.5 | 2 | l.PALI**S**WI**K**RKRQQ-$NH_2$ |
| b15 – $NH_3$ | 1374.6 | 1 | H-GIGAVLKVLTTGLPA.l | y10 | 922.8 | 2 | l.I**S**WI**K**RKRQQ-$NH_2$ |
| b16 | 753.7 | 2 | H-GIGAVLKVLTTGLPAL.i | y9 | 866.3 | 2 | i.**S**WI**K**RKRQQ-$NH_2$ |
| b17 | 809.8 | 2 | H-GIGAVLKVLTTGLPALI.s | y6 | 1080.6 | 1 | i.**K**RKRQQ-$NH_2$ |
| b18 | 985.0 | 2 | H-GIGAVLKVLTTGLPALIS.w | | | | |

¶ **Oleoylation** and **palmitoylation** sites within the amino acid sequence of the peptide are highlighted in **bold red** and **bold blue** respectively.

**Table S20. Ions produced by fragmenting melittin modified by 1 oleoyl group + 1 palmitoyl group at *m/z* 838 (*z* = 4) at RT = 9.1 min of the EIC (see Fig. 3 and Fig. S13), LTQFT. Data are presented graphically in Fig. S14b.**

| b-Ions | *m/z* | *z* | Sequence Ladder[¶] | y-Ions | *m/z* | *z* | Sequence Ladder[¶] |
|---|---|---|---|---|---|---|---|
| b4 | 299.2 | 1 | H-GIGA.v | y20 | 1419.9 | 2 | l.KVLTTGLPALI**S**WI**K**RKRQQ-$NH_2$ |
| b5 | 398.2 | 1 | H-GIGAV.l | y19 | 1355.7 | 2 | k.VLTTGLPALI**S**WI**K**RKRQQ-$NH_2$ |
| b6 | 511.3 | 1 | H-GIGAVL.k | y18 | 1306.5 | 2 | v.LTTGLPALI**S**WI**K**RKRQQ-$NH_2$ |
| b8 | 738.8 | 1 | H-GIGAVLKV.l | y17 | 1249.5 | 2 | l.TTGLPALI**S**WI**K**RKRQQ-$NH_2$ |
| b9 | 851.6 | 1 | H-GIGAVLKVL.t | y16 | 1199.0 | 2 | t.TGLPALI**S**WI**K**RKRQQ-$NH_2$ |
| b12 | 1110.8 | 1 | H-GIGAVLKVLTTG.l | y15 | 1148.7 | 2 | t.GLPALI**S**WI**K**RKRQQ-$NH_2$ |
| b13 | 1223.7 | 1 | H-GIGAVLKVLTTGL.p | y14 | 1119.2 | 2 | g.LPALI**S**WI**K**RKRQQ-$NH_2$ |
| b13 + $H_2O$ | 621.4 | 2 | H-GIGAVLKVLTTGL.p | y13 | 1063.5 | 2 | l.PALI**S**WI**K**RKRQQ-$NH_2$ |
| b15 – $NH_3$ | 1374.6 | 1 | H-GIGAVLKVLTTGLPA.l | y10 | 922.8 | 2 | l.I**S**WI**K**RKRQQ-$NH_2$ |
| b16 | 753.7 | 2 | H-GIGAVLKVLTTGLPAL.i | y9 | 866.3 | 2 | i.**S**WI**K**RKRQQ-$NH_2$ |
| b17 | 809.8 | 2 | H-GIGAVLKVLTTGLPALI.s | | | | |
| b18 | 971.9 | 2 | H-GIGAVLKVLTTGLPALIS.w | | | | |

[¶] **Oleoylation** and **palmitoylation** sites within the amino acid sequence of the peptide are highlighted in **bold red** and **bold blue** respectively.

**Table S21. Ions produced by fragmenting melittin modified by 1 oleoyl group + 1 palmitoyl group at *m/z* 838 (*z* = 4) at RT = 9.5 min of the EIC (see Fig. 3 and Fig. S13), LTQFT. Data are presented graphically in Fig. S15a.**

| b-Ions | *m/z* | *z* | Sequence Ladder[¶] | y-Ions | *m/z* | *z* | Sequence Ladder[¶] |
|---|---|---|---|---|---|---|---|
| b4 | 299.1 | 1 | H-GIGA.v | y20 | 1419.9 | 2 | l.KVLTTGLPALISWI**K**R**K**RQQ-$NH_2$ |
| b5 | 398.2 | 1 | H-GIGAV.l | y19 | 1355.8 | 2 | k.VLTTGLPALISWI**K**R**K**RQQ-$NH_2$ |
| b6 | 511.4 | 1 | H-GIGAVL.k | y18 | 1306.5 | 2 | v.LTTGLPALISWI**K**R**K**RQQ-$NH_2$ |
| b8 | 738.6 | 1 | H-GIGAVLKV.l | y17 | 1249.4 | 2 | l.TTGLPALISWI**K**R**K**RQQ-$NH_2$ |
| b9 | 851.5 | 1 | H-GIGAVLKVL.t | y16 | 1199.1 | 2 | t.TGLPALISWI**K**R**K**RQQ-$NH_2$ |
| b12 | 1110.8 | 1 | H-GIGAVLKVLTTG.l | y15 | 1148.4 | 2 | t.GLPALISWI**K**R**K**RQQ-$NH_2$ |
| b13 | 1223.6 | 1 | H-GIGAVLKVLTTGL.p | y14 | 1119.2 | 2 | g.LPALISWI**K**R**K**RQQ-$NH_2$ |
| b13 + $H_2O$ | 621.5 | 2 | H-GIGAVLKVLTTGL.p | y13 | 1063.5 | 2 | l.PALISWI**K**R**K**RQQ-$NH_2$ |
| b15 – $NH_3$ | 1374.6 | 1 | H-GIGAVLKVLTTGLPA.l | y10 | 923.3 | 2 | l.ISWI**K**R**K**RQQ-$NH_2$ |
| b19 | 947.1 | 2 | H-GIGAVLKVLTTGLPALISW.i | y9 | 866.1 | 2 | i.SWI**K**R**K**RQQ-$NH_2$ |
| b20 | 1002.7 | 2 | H-GIGAVLKVLTTGLPALISWI.k | y8 | 822.5 | 2 | s.WI**K**R**K**RQQ-$NH_2$ |
| | | | | y7 | 729.4 | 2 | w.I**K**R**K**RQQ-$NH_2$ |
| | | | | y5 | 476.7 | 2 | k.R**K**RQQ-$NH_2$ |
| | | | | y4 | 795.9 | 1 | r.**K**RQQ-$NH_2$ |

[¶] **Oleoylation** and **palmitoylation** sites within the amino acid sequence of the peptide are highlighted in **bold red** and **bold blue** respectively.

**Table S22. Ions produced by fragmenting melittin modified by 1 oleoyl group + 1 palmitoyl group at *m/z* 838 (*z* = 4) at RT = 9.5 min of the EIC (see Fig. 3 and Fig. S13), LTQFT. Data are presented graphically in Fig. S15b.**

| b-Ions | *m/z* | *z* | Sequence Ladder[¶] | y-Ions | *m/z* | *z* | Sequence Ladder[¶] |
|---|---|---|---|---|---|---|---|
| b4 | 299.2 | 1 | H-GIGA.v | y20 | 1419.9 | 2 | l.KVLTTGLPALISWI**K**R**K**RQQ-$NH_2$ |
| b5 | 398.2 | 1 | H-GIGAV.l | y19 | 1355.8 | 2 | k.VLTTGLPALISWI**K**R**K**RQQ-$NH_2$ |
| b6 | 511.4 | 1 | H-GIGAVL.k | y18 | 1306.5 | 2 | v.LTTGLPALISWI**K**R**K**RQQ-$NH_2$ |
| b8 | 738.6 | 1 | H-GIGAVLKV.l | y17 | 1249.4 | 2 | l.TTGLPALISWI**K**R**K**RQQ-$NH_2$ |
| b9 | 851.5 | 1 | H-GIGAVLKVL.t | y16 | 1199.0 | 2 | t.TGLPALISWI**K**R**K**RQQ-$NH_2$ |
| b12 | 1110.8 | 1 | H-GIGAVLKVLTTG.l | y15 | 1148.4 | 2 | t.GLPALISWI**K**R**K**RQQ-$NH_2$ |
| b13 | 1223.6 | 1 | H-GIGAVLKVLTTGL.p | y14 | 1119.2 | 2 | g.LPALISWI**K**R**K**RQQ-$NH_2$ |
| b13 + $H_2O$ | 621.5 | 2 | H-GIGAVLKVLTTGL.p | y13 | 1063.5 | 2 | l.PALISWI**K**R**K**RQQ-$NH_2$ |
| b15 – $NH_3$ | 1374.6 | 1 | H-GIGAVLKVLTTGLPA.l | y10 | 923.3 | 2 | l.ISWI**K**R**K**RQQ-$NH_2$ |
| b19 | 946.3 | 2 | H-GIGAVLKVLTTGLPALISW.i | y9 | 866.1 | 2 | i.SWI**K**R**K**RQQ-$NH_2$ |
| b20 | 1002.7 | 2 | H-GIGAVLKVLTTGLPALISWI.k | y8 | 822.5 | 2 | s.WI**K**R**K**RQQ-$NH_2$ |
| | | | | y7 | 729.4 | 2 | w.I**K**R**K**RQQ-$NH_2$ |
| | | | | y5 | 489.3 | 2 | k.R**K**RQQ-$NH_2$ |
| | | | | y4 | 411.8 | 1 | r.**K**RQQ-$NH_2$ |

[¶] **Oleoylation** and **palmitoylation** sites within the amino acid sequence of the peptide are highlighted in **bold red** and **bold blue** respectively.

**Table S23. Ions produced by fragmenting melittin modified by 1 oleoyl group + 1 palmitoyl group at *m/z* 838 (*z* = 4) at RT = 9.5 min of the EIC (see Fig. 3 and Fig. S13), LTQFT.**

| b-Ions | *m/z* | *z* | Sequence Ladder[¶] | y-Ions | *m/z* | *z* | Sequence Ladder[¶] |
|---|---|---|---|---|---|---|---|
| b3 | 492.3 | 1 | H-**G**IG.a | y19 | 1223.6 | 2 | k.VLTTGLPALISWI**K**RKRQQ-$NH_2$ |
| b4 | 563.3 | 1 | H-**G**IGA.v | y18 | 1174.2 | 2 | v.LTTGLPALISWI**K**RKRQQ-$NH_2$ |
| b5 | 662.3 | 1 | H-**G**IGAV.l | y17 | 1117.7 | 2 | l.TTGLPALISWI**K**RKRQQ-$NH_2$ |
| b5 + $H_2O$ | 679.1 | 1 | H-**G**IGAV.l | y16 | 1066.6 | 2 | t.TGLPALISWI**K**RKRQQ-$NH_2$ |
| b6 | 775.3 | 1 | H-**G**IGAVL.k | y15 | 1016.5 | 2 | t.GLPALISWI**K**RKRQQ-$NH_2$ |
| b8 | 1002.7 | 1 | H-**G**IGAVLKV.l | y14 | 987.9 | 2 | g.LPALISWI**K**RKRQQ-$NH_2$ |
| b9 | 1115.6 | 1 | H-**G**IGAVLKVL.t | y13 | 931.2 | 2 | l.PALISWI**K**RKRQQ-$NH_2$ |
| b10 | 1216.8 | 1 | H-**G**IGAVLKVLT.t | y12 | 882.9 | 2 | p.ALISWI**K**RKRQQ-$NH_2$ |
| b12 | 1374.7 | 1 | H-**G**IGAVLKVLTTG.l | y11 | 847.2 | 2 | a.LISWI**K**RKRQQ-$NH_2$ |
| b13 | 1487.8 | 1 | H-**G**IGAVLKVLTTGL.p | y10 | 790.6 | 2 | l.ISWI**K**RKRQQ-$NH_2$ |
| b13 - $H_2O$ | 1469.7 | 1 | H-**G**IGAVLKVLTTGL.p | y9 | 733.7 | 2 | i.SWI**K**RKRQQ-$NH_2$ |
| | | | | y7 | 597.1 | 2 | w.I**K**RKRQQ-$NH_2$ |
| | | | | y6 | 1080.1 | 1 | i.**K**RKRQQ-$NH_2$ |
| | | | | y4 | 558.4 | 1 | r.KRQQ-$NH_2$ |
| | | | | y4 - $NH_3$ | 541.9 | 1 | r.KRQQ-$NH_2$ |

[¶] **Oleoylation** and **palmitoylation** sites within the amino acid sequence of the peptide are highlighted in **bold red** and **bold blue** respectively.

**Table S24. Ions produced by fragmenting melittin modified by 1 oleoyl group + 1 palmitoyl group at *m/z* 838 (*z* = 4) at RT = 9.5 min of the EIC (see Fig. 3 and Fig. S13), LTQFT.**

| b-Ions | *m/z* | *z* | Sequence Ladder[¶] | y-Ions | *m/z* | *z* | Sequence Ladder[¶] |
|---|---|---|---|---|---|---|---|
| b3 | 466.3 | 1 | H-**G**IG.a | y21 | 1356.8 | 2 | v.LKVLTTGLPALISWI**K**RKRQQ-$NH_2$ |
| b4 | 537.1 | 1 | H-**G**IGA.v | y20 | 1299.9 | 2 | l.KVLTTGLPALISWI**K**RKRQQ-$NH_2$ |
| b5 | 636.5 | 1 | H-**G**IGAV.l | y19 | 1236.7 | 2 | k.VLTTGLPALISWI**K**RKRQQ-$NH_2$ |
| b6 | 749.2 | 1 | H-**G**IGAVL.k | y18 | 1187.5 | 2 | v.LTTGLPALISWI**K**RKRQQ-$NH_2$ |
| b8 | 976.6 | 1 | H-**G**IGAVLKV.l | y17 | 1130.5 | 2 | l.TTGLPALISWI**K**RKRQQ-$NH_2$ |
| b9 | 1089.6 | 1 | H-**G**IGAVLKVL.t | y16 | 1080.1 | 2 | t.TGLPALISWI**K**RKRQQ-$NH_2$ |
| b10 | 1190.8 | 1 | H-**G**IGAVLKVLT.t | y15 | 1029.1 | 2 | t.GLPALISWI**K**RKRQQ-$NH_2$ |
| b12 | 1348.8 | 1 | H-**G**IGAVLKVLTTG.l | y14 | 1000.9 | 2 | g.LPALISWI**K**RKRQQ-$NH_2$ |
| b12 - $H_2O$ | 1330.8 | 1 | H-**G**IGAVLKVLTTG.l | y13 | 944.4 | 2 | l.PALISWI**K**RKRQQ-$NH_2$ |
| b12 - $H_2O$ | 666.2 | 2 | H-**G**IGAVLKVLTTG.l | y12 | 896.7 | 2 | p.ALISWI**K**RKRQQ-$NH_2$ |
| b13 | 1461.7 | 1 | H-**G**IGAVLKVLTTGL.p | y10 | 803.2 | 2 | l.ISWI**K**RKRQQ-$NH_2$ |
| b13 - $H_2O$ | 1443.8 | 1 | H-**G**IGAVLKVLTTGL.p | y9 | 747.2 | 2 | i.SWI**K**RKRQQ-$NH_2$ |
| b18 | 972.3 | 2 | H-**G**IGAVLKVLTTGLPALIS.w | y8 | 703.8 | 2 | s.WI**K**RKRQQ-$NH_2$ |
| | | | | y7 | 609.1 | 1 | w.I**K**RKRQQ-$NH_2$ |
| | | | | y4 | 558.4 | 1 | r.KRQQ-$NH_2$ |
| | | | | y4 – $NH_3$ | 541.9 | 1 | r.KRQQ-$NH_2$ |

[¶] **Oleoylation** and **palmitoylation** sites within the amino acid sequence of the peptide are highlighted in **bold red** and **bold blue** respectively.

**Table S25. Ions produced by fragmenting melittin modified by 1 oleoyl group + 1 palmitoyl group at *m/z* 838 (*z* = 4) at RT = 10.2 min of the EIC (see Fig. 3 and Fig. S13), LTQFT. Data are presented graphically in Fig. S16a.**

| b-Ions | *m/z* | *z* | Sequence Ladder[¶] | y-Ions | *m/z* | *z* | Sequence Ladder[¶] |
|---|---|---|---|---|---|---|---|
| b4 | 299.1 | 1 | H-GIGA.v | y21 | 1476.2 | 2 | v.LKVLTTGLPALISWI**K**RKRQQ-$NH_2$ |
| b5 | 398.2 | 1 | H-GIGAV.l | y20 | 1419.9 | 2 | l.KVLTTGLPALISWI**K**RKRQQ-$NH_2$ |
| b6 | 511.3 | 1 | H-GIGAVL.k | y19 | 1223.6 | 2 | k.VLTTGLPALISWI**K**RKRQQ-$NH_2$ |
| b7 | 903.6 | 1 | H-GIGAVL**K**.v | y18 | 1174.0 | 2 | v.LTTGLPALISWI**K**RKRQQ-$NH_2$ |
| b8 | 1002.6 | 1 | H-GIGAVL**K**V.l | y17 | 1117.4 | 2 | l.TTGLPALISWI**K**RKRQQ-NH2 |
| b9 | 1115.7 | 1 | H-GIGAVL**K**VL.t | y16 | 1067.3 | 2 | t.TGLPALISWI**K**RKRQQ-$NH_2$ |
| b10 | 1216.7 | 1 | H-GIGAVL**K**VLT.t | y15 | 1016.4 | 2 | t.GLPALISWI**K**RKRQQ-$NH_2$ |
| b10 - $H_2O$ | 1198.9 | 1 | H-GIGAVL**K**VLT.t | y14 | 987.6 | 2 | g.LPALISWI**K**RKRQQ-$NH_2$ |
| b11 | 1317.7 | 1 | H-GIGAVL**K**VLTT.g | y13 | 931.1 | 2 | l.PALISWI**K**RKRQQ-$NH_2$ |
| b12 | 1374.7 | 1 | H-GIGAVL**K**VLTTG.l | y9 | 733.5 | 2 | i.SWI**K**RKRQQ-$NH_2$ |
| b12 - $H_2O$ | 1356.6 | 1 | H-GIGAVL**K**VLTTG.l | y7 | 597.5 | 2 | w.I**K**RKRQQ-$NH_2$ |
| b12 - $H_2O$ | 678.1 | 2 | H-GIGAVL**K**VLTTG.l | y6 | 1080.5 | 1 | i.**K**RKRQQ-$NH_2$ |
| b13 | 1488.0 | 1 | H-GIGAVL**K**VLTTGL.p | y6 | 540.9 | 2 | i.**K**RKRQQ-$NH_2$ |
| b13 - $H_2O$ | 1470.1 | 1 | H-GIGAVL**K**VLTTGL.p | y6 - $NH_3$ | 1063.5 | 1 | i.**K**RKRQQ-$NH_2$ |
| b14 - $H_2O$ | 783.2 | 2 | H-GIGAVL**K**VLTTGLP.a | y4 | 558.3 | 1 | r.KRQQ-$NH_2$ |
| b18 | 985.1 | 2 | H-GIGAVL**K**VLTTGLPALIS.w | | | | |

[¶] **Oleoylation** and **palmitoylation** sites within the amino acid sequence of the peptide are highlighted in **bold red** and **bold blue** respectively.

**Table S26. Ions produced by fragmenting melittin modified by 1 oleoyl group + 1 palmitoyl group at *m/z* 838 (*z* = 4) at RT = 10.2 min of the EIC (see Fig. 3 and Fig. S13), LTQFT. Data are presented graphically in Fig. S16b.**

| b-Ions | *m/z* | *z* | Sequence Ladder[¶] | y-Ions | *m/z* | *z* | Sequence Ladder[¶] |
|---|---|---|---|---|---|---|---|
| b4 | 299.1 | 1 | H-GIGA.v | y21 | 1476.2 | 2 | v.LKVLTTGLPALISWI**K**RKRQQ-$NH_2$ |
| b5 | 398.2 | 1 | H-GIGAV.l | y20 | 1419.9 | 2 | l.KVLTTGLPALISWI**K**RKRQQ-$NH_2$ |
| b6 | 511.3 | 1 | H-GIGAVL.k | y19 | 1236.6 | 2 | k.VLTTGLPALISWI**K**RKRQQ-$NH_2$ |
| b7 | 877.5 | 1 | H-GIGAVL**K**.v | y18 | 1187.2 | 2 | v.LTTGLPALISWI**K**RKRQQ-$NH_2$ |
| b8 | 976.6 | 1 | H-GIGAVL**K**V.l | y17 | 1130.3 | 2 | l.TTGLPALISWI**K**RKRQQ-$NH_2$ |
| b9 | 1089.6 | 1 | H-GIGAVL**K**VL.t | y16 | 1080.0 | 2 | t.TGLPALISWI**K**RKRQQ-$NH_2$ |
| b10 | 1190.7 | 1 | H-GIGAVL**K**VLT.t | y15 | 1030.1 | 2 | t.GLPALISWI**K**RKRQQ-$NH_2$ |
| b11 | 1291.7 | 1 | H-GIGAVL**K**VLTT.g | y14 | 1000.7 | 2 | g.LPALISWI**K**RKRQQ-$NH_2$ |
| b11 - $H_2O$ | 1273.7 | 1 | H-GIGAVL**K**VLTT.g | y13 | 944.3 | 2 | l.PALISWI**K**RKRQQ-$NH_2$ |
| b12 | 1348.6 | 1 | H-GIGAVL**K**VLTTG.l | y12 | 896.4 | 2 | p.ALISWI**K**RKRQQ-$NH_2$ |
| b12 - $H_2O$ | 1330.8 | 1 | H-GIGAVL**K**VLTT G.l | y11 | 860.0 | 2 | a.LISWI**K**RKRQQ-$NH_2$ |
| b12 - $H_2O$ | 665.9 | 2 | H-GIGAVL**K**VLTT G.l | y10 | 803.2 | 2 | l.ISWI**K**RKRQQ-$NH_2$ |
| b13 | 1461.8 | 1 | H-GIGAVL**K**VLTTGL.p | y9 | 745.9 | 2 | i.SWI**K**RKRQQ-$NH_2$ |
| b15 | 816.1 | 2 | H-GIGAVL**K**VLTTGLPA.l | y8 | 703.5 | 2 | s.WI**K**RKRQQ-$NH_2$ |
| b18 | 972.4 | 2 | H-GIGAVL**K**VLTTGLPALIS.w | y7 | 610.5 | 2 | w.I**K**RKRQQ-$NH_2$ |
| | | | | y4 | 558.3 | 2 | r.KRQQ-$NH_2$ |

[¶] **Oleoylation** and **palmitoylation** sites within the amino acid sequence of the peptide are highlighted in **bold red** and **bold blue** respectively.

**Table S27. Ions produced by fragmenting melittin modified by 1 oleoyl group + 1 palmitoyl group at *m/z* 838 (*z* = 4) at RT = 10.6 min of the EIC (see Fig. 3 and Fig. S13), LTQFT. Data are presented graphically in Fig. S17a.**

| b-Ions | *m/z* | *z* | Sequence Ladder[¶] | y-Ions | *m/z* | *z* | Sequence Ladder[¶] |
|---|---|---|---|---|---|---|---|
| b3 | 492.3 | 1 | H-**G**IG.a | y19 | 1223.6 | 2 | k.VLTTGLPALISWIKR**K**RQQ-$NH_2$ |
| b4 | 563.3 | 1 | H-**G**IGA.v | y18 | 1173.9 | 2 | v.LTTGLPALISWIKR**K**RQQ-$NH_2$ |
| b5 | 662.3 | 1 | H-**G**IGAV.l | y17 | 1117.8 | 2 | l.TTGLPALISWIKR**K**RQQ-$NH_2$ |
| b5 + $H_2O$ | 679.2 | 1 | H-**G**IGAV.l | y16 | 1067.0 | 2 | t.TGLPALISWIKR**K**RQQ-$NH_2$ |
| b6 | 775.3 | 1 | H-**G**IGAVL.k | y15 | 1016.3 | 2 | t.GLPALISWIKR**K**RQQ-$NH_2$ |
| b8 | 1002.6 | 1 | H-**G**IGAVLKV.l | y14 | 988.0 | 2 | g.LPALISWIKR**K**RQQ-$NH_2$ |
| b9 | 1115.6 | 1 | H-**G**IGAVLKVL.t | y13 | 931.4 | 2 | l.PALISWIKR**K**RQQ-$NH_2$ |
| b10 | 1216.8 | 1 | H-**G**IGAVLKVLT.t | y12 | 882.9 | 2 | p.ALISWIKR**K**RQQ-$NH_2$ |
| b12 | 1374.7 | 1 | H-**G**IGAVLKVLTTG.l | y11 | 847.3 | 2 | a.LISWIKR**K**RQQ-$NH_2$ |
| b13 | 1487.7 | 1 | H-**G**IGAVLKVLTTGL.p | y10 | 790.5 | 2 | l.ISWIKR**K**RQQ-$NH_2$ |
| b13 - $H_2O$ | 1470.1 | 1 | H-**G**IGAVLKVLTTGL.p | y9 | 734.0 | 2 | i.SWIKR**K**RQQ-$NH_2$ |
| | | | | y8 | 690.8 | 2 | s.WIKR**K**RQQ-$NH_2$ |
| | | | | y7 | 598.6 | 2 | w.IKR**K**RQQ-$NH_2$ |
| | | | | y6 | 1080.3 | 1 | i.KR**K**RQQ-$NH_2$ |
| | | | | y5 | 952.9 | 1 | k.R**K**RQQ-$NH_2$ |
| | | | | y5 | 476.9 | 2 | k.R**K**RQQ-$NH_2$ |
| | | | | y4 | 796.4 | 1 | r.**K**RQQ-$NH_2$ |
| | | | | y4 - $NH_3$ | 779.7 | 1 | r.**K**RQQ-$NH_2$ |

[¶] **Oleoylation** and **palmitoylation** sites within the amino acid sequence of the peptide are highlighted in **bold red** and **bold blue** respectively.

**Table S28. Ions produced by fragmenting melittin modified by 1 oleoyl group + 1 palmitoyl group at *m/z* 838 (*z* = 4) at RT = 10.6 min of the EIC (see Fig. 3 and Fig. S13), LTQFT. Data are presented graphically in Fig. S17b.**

| b-Ions | *m/z* | *z* | Sequence Ladder[¶] | y-Ions | *m/z* | *z* | Sequence Ladder[¶] |
|---|---|---|---|---|---|---|---|
| b3 | 466.3 | 1 | H-**G**IG.a | y21 | 1356.7 | 2 | v.LKVLTTGLPALISWI**K**RKRQQ-$NH_2$ |
| b4 | 537.2 | 1 | H-**G**IGA.v | y20 | 1299.9 | 2 | l.KVLTTGLPALISWIKR**K**RQQ-$NH_2$ |
| b5 | 636.2 | 1 | H-**G**IGAV.l | y19 | 1236.5 | 2 | k.VLTTGLPALISWIKR**K**RQQ-$NH_2$ |
| b6 | 749.1 | 1 | H-**G**IGAVL.k | y18 | 1186.8 | 2 | v.LTTGLPALISWIKR**K**RQQ-$NH_2$ |
| b7 | 877.4 | 1 | H-**G**IGAVLK.v | y17 | 1130.6 | 2 | l.TTGLPALISWIKR**K**RQQ-$NH_2$ |
| b8 | 976.6 | 1 | H-**G**IGAVLKV.l | y16 | 1080.1 | 2 | t.TGLPALISWIKR**K**RQQ-$NH_2$ |
| b9 | 1089.7 | 1 | H-**G**IGAVLKVL.t | y15 | 1029.5 | 2 | t.GLPALISWIKR**K**RQQ-$NH_2$ |
| b10 | 1190.2 | 1 | H-**G**IGAVLKVLT.t | y14 | 1001.0 | 2 | g.LPALISWIKR**K**RQQ-$NH_2$ |
| b12 | 1348.6 | 1 | H-**G**IGAVLKVLTTG.l | y13 | 944.4 | 2 | l.PALISWIKR**K**RQQ-$NH_2$ |
| b12 - $H_2O$ | 1330.8 | 1 | H-**G**IGAVLKVLTTG.l | y12 | 896.6 | 2 | p.ALISWIKR**K**RQQ-$NH_2$ |
| b12 - $H_2O$ | 666.1 | 2 | H-**G**IGAVLKVLTTG.l | y11 | 860.4 | 2 | a.LISWIKR**K**RQQ-$NH_2$ |
| b13 | 1461.7 | 1 | H-**G**IGAVLKVLTTGL.p | y10 | 803.7 | 2 | l.ISWIKR**K**RQQ-$NH_2$ |
| b13 - $H_2O$ | 1443.7 | 1 | H-**G**IGAVLKVLTTGL.p | y9 | 746.7 | 2 | i.SWIKR**K**RQQ-$NH_2$ |
| b18 | 972.3 | 2 | H-**G**IGAVLKVLTTGLPALIS.w | y7 | 703.8 | 2 | w.IKR**K**RQQ-$NH_2$ |
| | | | | y5 | 609.1 | 2 | k.R**K**RQQ-$NH_2$ |
| | | | | y4 | 822.6 | 1 | r.**K**RQQ-$NH_2$ |
| | | | | y4 | 411.4 | 2 | r.**K**RQQ-$NH_2$ |

[¶] **Oleoylation** and **palmitoylation** sites within the amino acid sequence of the peptide are highlighted in **bold red** and **bold blue** respectively.

**Table S29. Ions produced by fragmenting melittin modified by 1 oleoyl group + 1 palmitoyl group at *m/z* 838 (*z* = 4) at RT = 10.9 min of the EIC (see Fig. 3 and Fig. S13), LTQFT. Data are presented graphically in Fig. S18a.**

| b-Ions | *m/z* | *z* | Sequence Ladder[¶] | y-Ions | *m/z* | *z* | Sequence Ladder[¶] |
|---|---|---|---|---|---|---|---|
| b3 | 492.3 | 1 | H-**G**IG.a | y19 | 1223.6 | 2 | k.VLTTGLPALISWIK**R**KRQQ-$NH_2$ |
| b4 | 563.2 | 1 | H-**G**IGA.v | y18 | 1173.8 | 2 | v.LTTGLPALISWIK**R**KRQQ-$NH_2$ |
| b5 | 662.3 | 1 | H-**G**IGAV.l | y17 | 1117.9 | 2 | l.TTGLPALISWIK**R**KRQQ-$NH_2$ |
| b5 + $H_2O$ | 679.0 | 1 | H-**G**IGAV.l | y16 | 1067.1 | 2 | t.TGLPALISWIK**R**KRQQ-$NH_2$ |
| b6 | 775.3 | 1 | H-**G**IGAVL.k | y15 | 1016.5 | 2 | t.GLPALISWIK**R**KRQQ-$NH_2$ |
| b8 | 1002.5 | 1 | H-**G**IGAVLKV.l | y14 | 988.1 | 2 | g.LPALISWIK**R**KRQQ-$NH_2$ |
| b9 | 1115.7 | 1 | H-**G**IGAVLKVL.t | y13 | 931.4 | 2 | l.PALISWIK**R**KRQQ-$NH_2$ |
| b10 | 1216.7 | 1 | H-**G**IGAVLKVLT.t | y12 | 882.8 | 2 | p.ALISWIK**R**KRQQ-$NH_2$ |
| b12 | 1374.7 | 1 | H-**G**IGAVLKVLTTG.l | y11 | 847.3 | 2 | a.LISWIK**R**KRQQ-$NH_2$ |
| b13 | 1487.7 | 1 | H-**G**IGAVLKVLTTGL.p | y10 | 790.4 | 2 | l.ISWIK**R**KRQQ-$NH_2$ |
| b13 – $H_2O$ | 1470.2 | 1 | H-**G**IGAVLKVLTTGL.p | y9 | 734.1 | 2 | i.SWIK**R**KRQQ-$NH_2$ |
| | | | | y8 | 690.7 | 2 | s.WIK**R**KRQQ-$NH_2$ |
| | | | | y7 | 598.6 | 2 | w.IK**R**KRQQ-$NH_2$ |
| | | | | y6 | 1080.1 | 1 | i.K**R**KRQQ-$NH_2$ |
| | | | | y5 | 953.2 | 1 | k.**R**KRQQ-$NH_2$ |
| | | | | y4 | 558.6 | 1 | r.KRQQ-$NH_2$ |
| | | | | y4 - $NH_3$ | 541.3 | 1 | r.KRQQ-$NH_2$ |

[¶] **Oleoylation** and **palmitoylation** sites within the amino acid sequence of the peptide are highlighted in **bold red** and **bold blue** respectively.

**Table S30. Ions produced by fragmenting melittin modified by 1 oleoyl group + 1 palmitoyl group at *m/z* 838 (*z* = 4) at RT = 10.9 min of the EIC (see Fig. 3 and Fig. S13), LTQFT. Data are presented graphically in Fig. S18b.**

| b-Ions | *m/z* | *z* | Sequence Ladder[¶] | y-Ions | *m/z* | *z* | Sequence Ladder[¶] |
|---|---|---|---|---|---|---|---|
| b3 | 466.3 | 1 | H-**G**IG.a | y21 | 1356.7 | 2 | v.LKVLTTGLPALISWIK**R**KRQQ-$NH_2$ |
| b4 | 537.2 | 1 | H-**G**IGA.v | y18 | 1186.9 | 2 | v.LTTGLPALISWIK**R**KRQQ-$NH_2$ |
| b5 | 636.2 | 1 | H-**G**IGAV.l | y17 | 1130.5 | 2 | l.TTGLPALISWIK**R**KRQQ-$NH_2$ |
| b6 | 749.3 | 1 | H-**G**IGAVL.k | y16 | 1080.1 | 2 | t.TGLPALISWIK**R**KRQQ-$NH_2$ |
| b7 | 877.4 | 1 | H-**G**IGAVLK.v | y15 | 1029.5 | 2 | t.GLPALISWIK**R**KRQQ-$NH_2$ |
| b8 | 976.6 | 1 | H-**G**IGAVLKV.l | y14 | 1000.8 | 2 | g.LPALISWIK**R**KRQQ-$NH_2$ |
| b9 | 1089.6 | 1 | H-**G**IGAVLKVL.t | y13 | 944.4 | 2 | l.PALISWIK**R**KRQQ-$NH_2$ |
| b12 - $H_2O$ | 1330.8 | 1 | H-**G**IGAVLKVLTTG.l | y12 | 896.4 | 2 | p.ALISWIK**R**KRQQ-$NH_2$ |
| b12 - $H_2O$ | 666.0 | 2 | H-**G**IGAVLKVLTTG.l | y11 | 860.4 | 2 | a.LISWIK**R**KRQQ-$NH_2$ |
| b18 | 972.2 | 2 | H-**G**IGAVLKVLTTGLPALIS.w | y10 | 803.7 | 2 | l.ISWIK**R**KRQQ-$NH_2$ |
| | | | | y9 | 747.2 | 2 | i.SWIK**R**KRQQ-$NH_2$ |
| | | | | y8 | 703.8 | 2 | s.WIK**R**KRQQ-$NH_2$ |
| | | | | y7 | 609.1 | 2 | w.IK**R**KRQQ-$NH_2$ |
| | | | | y5 | 978.8 | 1 | k.**R**KRQQ-$NH_2$ |
| | | | | y5 | 489.9 | 1 | k.**R**KRQQ-$NH_2$ |
| | | | | y4 | 558.3 | 1 | r.KRQQ-$NH_2$ |
| | | | | y4 - $NH_3$ | 541.1 | 1 | r.KRQQ-$NH_2$ |

[¶] **Oleoylation** and **palmitoylation** sites within the amino acid sequence of the peptide are highlighted in **bold red** and **bold blue** respectively.

**Table S31. Ions produced by fragmenting melittin modified by 1 oleoyl group + 1 palmitoyl group at *m/z* 838 (*z* = 4) at RT = 11.2 min of the EIC (see Fig. 3 and Fig. S13), LTQFT. Data are presented graphically in Fig. S19a.**

| b-Ions | *m/z* | *z* | Sequence Ladder[¶] | y-Ions | *m/z* | *z* | Sequence Ladder[¶] |
|---|---|---|---|---|---|---|---|
| b3 | 492.2 | 1 | H-**G**IG.a | y19 | 1223.7 | 2 | k.VLTTGLPALISWIKRK**R**QQ-$NH_2$ |
| b4 | 563.2 | 1 | H-**G**IGA.v | y18 | 1174.2 | 2 | v.LTTGLPALISWIKRK**R**QQ-$NH_2$ |
| b5 | 662.4 | 1 | H-**G**IGAV.l | y17 | 1117.7 | 2 | l.TTGLPALISWIKRK**R**QQ-$NH_2$ |
| b5 + $H_2O$ | 679.1 | 1 | H-**G**IGAV.l | y16 | 1066.9 | 2 | t.TGLPALISWIKRK**R**QQ-$NH_2$ |
| b6 | 775.2 | 1 | H-**G**IGAVL.k | y15 | 1016.4 | 2 | t.GLPALISWIKRK**R**QQ-$NH_2$ |
| b8 | 1002.6 | 1 | H-**G**IGAVLKV.l | y14 | 988.0 | 2 | g.LPALISWIKRK**R**QQ-$NH_2$ |
| b9 | 1115.6 | 1 | H-**G**IGAVLKVL.t | y13 | 931.5 | 2 | l.PALISWIKRK**R**QQ-$NH_2$ |
| b10 | 1216.7 | 1 | H-**G**IGAVLKVLT.t | y12 | 882.8 | 2 | p.ALISWIKRK**R**QQ-$NH_2$ |
| b12 | 1374.7 | 1 | H-**G**IGAVLKVLTTG.l | y11 | 847.2 | 2 | a.LISWIKRK**R**QQ-$NH_2$ |
| b13 | 1487.7 | 1 | H-**G**IGAVLKVLTTGL.p | y10 | 790.8 | 2 | l.ISWIKRK**R**QQ-$NH_2$ |
| b13 – $H_2O$ | 1469.8 | 1 | H-**G**IGAVLKVLTTGL.p | y9 | 734.2 | 2 | i.SWIKRK**R**QQ-$NH_2$ |
| | | | | y8 | 690.8 | 2 | s.WIKRK**R**QQ-$NH_2$ |
| | | | | y7 | 598.0 | 2 | w.IKRK**R**QQ-$NH_2$ |
| | | | | y6 | 1080.1 | 1 | i.KRK**R**QQ-$NH_2$ |
| | | | | y5 | 953.2 | 1 | k.RK**R**QQ-$NH_2$ |
| | | | | y4 | 796.1 | 1 | r.K**R**QQ-$NH_2$ |
| | | | | y4 - $NH_3$ | 779.5 | 1 | r.K**R**QQ-$NH_2$ |

[¶] **Oleoylation** and **palmitoylation** sites within the amino acid sequence of the peptide are highlighted in **bold red** and **bold blue** respectively.

**Table S32. Ions produced by fragmenting melittin modified by 1 oleoyl group + 1 palmitoyl group at *m/z* 838 (*z* = 4) at RT = 11.2 min of the EIC (see Fig. 3 and Fig. S13), LTQFT. Data are presented graphically in Fig. S19b.**

| b-Ions | *m/z* | *z* | Sequence Ladder[¶] | y-Ions | *m/z* | *z* | Sequence Ladder[¶] |
|---|---|---|---|---|---|---|---|
| b3 | 466.3 | 1 | H-**G**IG.a | y21 | 1356.8 | 2 | v.LKVLTTGLPALISWIKRK**R**QQ-$NH_2$ |
| b4 | 537.2 | 1 | H-**G**IGA.v | y19 | 1236.5 | 2 | k.VLTTGLPALISWIKRK**R**QQ-$NH_2$ |
| b5 | 636.4 | 1 | H-**G**IGAV.l | y18 | 1186.5 | 2 | v.LTTGLPALISWIKRK**R**QQ-$NH_2$ |
| b6 | 749.8 | 1 | H-**G**IGAVL.k | y17 | 1130.4 | 2 | l.TTGLPALISWIKRK**R**QQ-$NH_2$ |
| b7 | 877.7 | 1 | H-**G**IGAVLK.v | y16 | 1079.7 | 2 | t.TGLPALISWIKRK**R**QQ-$NH_2$ |
| b8 | 976.6 | 1 | H-**G**IGAVLKV.l | y15 | 1029.1 | 2 | t.GLPALISWIKRK**R**QQ-$NH_2$ |
| b9 | 1089.6 | 1 | H-**G**IGAVLKVL.t | y14 | 1000.7 | 2 | g.LPALISWIKRK**R**QQ-$NH_2$ |
| b10 | 1190.1 | 1 | H-**G**IGAVLKVLT.t | y13 | 944.5 | 2 | l.PALISWIKRK**R**QQ-$NH_2$ |
| b12 | 1348.7 | 1 | H-**G**IGAVLKVLTTG.l | y12 | 896.0 | 2 | p.ALISWIKRK**R**QQ-$NH_2$ |
| b12 - $H_2O$ | 1330.6 | 1 | H-**G**IGAVLKVLTTG.l | y11 | 860.5 | 2 | a.LISWIKRK**R**QQ-$NH_2$ |
| b12 - $H_2O$ | 665.8 | 2 | H-**G**IGAVLKVLTTG.l | y10 | 803.9 | 2 | l.ISWIKRK**R**QQ-$NH_2$ |
| b13 | 1462.2 | 1 | H-**G**IGAVLKVLTTGL.p | y9 | 746.8 | 2 | i.SWIKRK**R**QQ-$NH_2$ |
| b13 - $H_2O$ | 1443.9 | 1 | H-**G**IGAVLKVLTTGL.p | y8 | 703.8 | 2 | s.WIK**R**QQ-$NH_2$ |
| b18 | 972.3 | 2 | H-**G**IGAVLKVLTTGLPALIS.w | y5 | 489.9 | 2 | k.RK**R**QQ-$NH_2$ |
| | | | | y4 | 822.6 | 1 | r.K**R**QQ-$NH_2$ |

[¶] **Oleoylation** and **palmitoylation** sites within the amino acid sequence of the peptide are highlighted in **bold red** and **bold blue** respectively.

## References


1 C. J. Van Echteld, B. de Kruijff, J. G. Mandersloot and J. De Gier, *Biochim. Biophys. Acta*, 1981, **649**, 211–220.

2 J. R. Henriksen, T. L. Andresen, L. N. Feldborg, L. Duelund and J. H. Ipsen, *Biophys. J.*, 2010, **98**, 2199–2205.

3 D. V. Zhelev, *Biophys. J.*, 1998, **75**, 321–330.

4 D. Needham and D. V. Zhelev, *Ann. Biomed. Eng.*, 1995, **23**, 287–298.